Pattern Recognition ■ (■■■■) ■■■–■■■

Contents lists available at ScienceDirect

Pattern Recognition

journal homepage: www.elsevier.com/locate/pr

# A survey of Hough Transform

Priyanka Mukhopadhyay [a,b,*], Bidyut B. Chaudhuri [a]

[a] Department of Computer Science (Centre for Vision and Pattern Recognition (CVPR)), Indian Statistical Institute, Kolkata, India
[b] National University of Singapore, Singapore

ARTICLE INFO

*Article history:*
Received 22 November 2013
Received in revised form
20 July 2014
Accepted 31 August 2014

*Keywords:*
Hough Transform (HT)
Generalized Hough Transform (GHT)
Probabilistic Hough Transform (PHT)
Randomized Hough Transform (RHT)
Digital Hough Transform (DHT)

ABSTRACT

In 1962 Hough earned the patent for a method [1], popularly called Hough Transform (HT) that efficiently identifies lines in images. It is an important tool even after the golden jubilee year of existence, as evidenced by more than 2500 research papers dealing with its variants, generalizations, properties and applications in diverse fields. The current paper is a survey of HT and its variants, their limitations and the modifications made to overcome them, the implementation issues in software and hardware, and applications in various fields. Our survey, along with more than 200 references, will help the researchers and students to get a comprehensive view on HT and guide them in applying it properly to their problems of interest.

© 2014 Elsevier Ltd. All rights reserved.

## 1. Introduction

One of the challenges of automated digital image analysis is shape detection, which is an important part of object recognition. Unfortunately, direct searching and detection of a class of even simple geometric patterns like straight lines, circles and ellipses in an image are very computation intensive. Besides, occlusion of curves or missing and spurious data pixels due to noise arising from either the imperfection of image data or edge detector makes this task non-trivial. To address this problem, nearly 50 years ago, Hough [1] while trying to detect and plot the tracks of subatomic particles in bubble chamber photographs, devised the Hough Transform (HT), an ingenious method that converts such global curve detection problem into an efficient peak detection problem in parameter space. Rosenfeld [2] popularized it in main stream computer vision society by giving the first algebraic form for the transform and proposed a simple digital implementation of the transform space as an array of counters. An interesting history about the invention of HT has been narrated in Hart [188].

For illustration, consider the problem of detecting straight lines for which Hough chose the slope-intercept parametric equation of line:

$$f(x,y) = y - mx - c = 0 \tag{1}$$

where the parameters $m$ and $c$ are the slope and $y$-intercept of the line respectively. The transformation is done on a binary image, obtained after processing the original image by an edge detector. The parameter space is quantized in intervals of $\Delta m$ and $\Delta c$ and corresponding bins are created to collect the evidence (or vote) of object pixels satisfying Eq. (1). Consider the $(k, n)$th bin corresponding to intervals $[(k-1)\Delta m, k\,\Delta m)$ and $[(n-1)\Delta c, n\,\Delta c)$ where $k, n \in \mathbb{Z}^+$. For each object pixel satisfying Eq. (1) with parameters in the above range, the vote in the $(k, n)$th bin is incremented by 1. In the peak detection phase, the bins having number of votes above a critical threshold correspond to straight lines in the image. This set of bins is also called the accumulator. A more precise definition of accumulator will be given in Section 4.5.

This approach can also be extended to any parametric analytic curve with expression $f(\mathbf{X}, \mathbf{a}) = 0$ where $\mathbf{X} \in \mathbb{R}^d$ is the variable co-ordinate vector and $\mathbf{a} \in \mathbb{R}^n$ denote the constant parameter vector. Its dual (projection equation) in the parameter space may be expressed as $g(\mathbf{a}, \mathbf{X}) = 0$ where $\mathbf{a}$ is the variable parameter vector and $\mathbf{X}$ is the constant co-ordinate vector. Thus, the intersection point of the $n$ hypersurfaces defined by the projection equations determines the parameters of the given curve. This approach limited to parametric analytic curve detection is usually referred to as the Standard Hough Transform (SHT) (Fig. 1).

Two comprehensive surveys of the HT have been made in the past [34,77]. But newer studies are being conducted continuously on this topic, newer implementations are being proposed and applications in various fields are being researched. Since 2012 was the golden jubilee year of the patent granted to Hough, we planned to prepare another survey on HT. Available literature on HT is quite vast. So it was not possible for us to cover every aspect with equal depth keeping in mind space constraints. We have tried to state and elaborate a bit on the aspects we thought were

* Corresponding author. Current address: National University of Singapore, Singapore
*E-mail addresses:* mukhopadhyay.priyanka@gmail.com (P. Mukhopadhyay), bbcisical@gmail.com (B.B. Chaudhuri).

http://dx.doi.org/10.1016/j.patcog.2014.08.027
0031-3203/© 2014 Elsevier Ltd. All rights reserved.

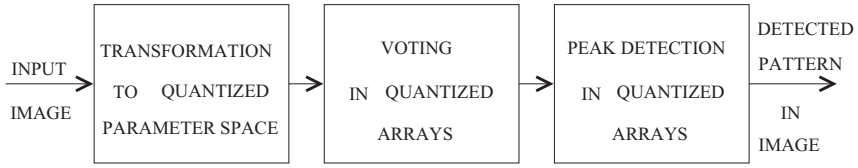


**Fig. 1.** Block diagram of HT for parameterized curves.

important and we sincerely hope that it benefits the students and research community on this useful tool. We start by discussing the various HT formulations in Section 2 before describing its major variants in Section 3. In Section 4 we discuss various limitations of HT and the modifications made to overcome them. Section 5 deals with implementation issues, while in Section 6 we discuss in brief a few applications of HT in some selected fields.

## 2. Formulation

Since straight line detection is the most popular and widely studied application of HT, we begin this section with some of its parametric formulations.

### 2.1. Straight line parameterization

The slope-intercept form discussed in Section 1 is one of the earliest parametric forms used for straight line detection. The dual of Eq. (1) is also that of a straight line:

$$g(m,c)=y'-mx'-c=0 \tag{2}$$

where $(x',y')$ is the co-ordinate of the pixel being mapped. Since collinear pixels in image space are mapped to concurrent straight lines in the parameter space, this approach is a Point-to-Line Mapping (PTLM). Unfortunately, this method is sensitive to the choice of co-ordinate axes on the image plane because both the parameters become unbounded when the detectable line is at $\pi/2$ with respect to the abscissa. In fact, Bhattacharya et al. [137] have shown that any one-to-one PTLM must be linear and cannot map all the sets of collinear points lying in a bounded region (such as an image) into sets of concurrent lines intersecting on a bounded region. Hence if such a PTLM defines an HT, it cannot be practical to search for all the accumulator peaks. This problem can be tackled by defining a second parameter space, rotated from the first by 90°, as envisioned by Rosenfeld [2]. Somewhat on the same line, Tuytelaars et al. [115] proposed a variant by splitting the $(m, c)$ space into three bounded subspaces.

Duda and Hart [3] lucidly resolved the issue of unboundedness by mapping a point in image space to a sinusoidal curve in parameter space:

$$f(x,y)=\rho(\theta)=x\ \cos\ (\theta)+y\ \sin\ (\theta) \tag{3}$$

This function has period $2\pi$ and obeys the relation

$$\rho(\theta)=-\rho(\theta+\pi) \tag{4}$$

A parameter subspace is redundant if it contains points, which can be mapped to each other using this relation. Immerkaer [112] has shown that the parameter subspace $(\theta,\rho)\in[0,\pi[\times]-\infty,\infty[$ is non-redundant and sufficient to construct the entire parameter space. Memory requirement of the accumulator array is reduced to 59% when the image center, instead of corner, is used as the origin.

Other features can also be used for mapping like the foot of normal from a chosen origin [22] and the neighborhood of a straight line [194]. The former maps to a space congruent to the image space and does not require the computation of trigonometric functions, thus saving time. Unlike SHT, which puts more emphasis on parameter domain resolutions, the latter represents the image space resolution explicitly.

### 2.2. Parameterization for circle and ellipse detection

Often in image analysis, the detection of circles and ellipses before the objects themselves is profitable. A significant portion of man-made and natural objects has a circular profile like disc, coin, button, celestial body, biscuit, and biological part. Oblique projection of these objects makes elliptical shape on a 2-D space. The ellipse parameters give an estimate of the relative orientation between the object and the camera.

The parameterization of circle used in [1,3] is

$$f_c(x,y)=(x-a)^2+(y-b)^2-r^2=0 \tag{5}$$

where $(a, b)$ denote the center and $r$ is the radius of the circle. Thus each pixel in the image plane is transformed to a cone (Fig. 3) in a 3-D parameter space.

This process is also known as the Circle HT (CHT) [87]. Kerbyson and Atherton [87] show that a substantial improvement in positional accuracy can be achieved by using orientation and distance information coded as a complex phase.

The general equation of an ellipse is

$$x^2+b'y^2+2d'xy+2e'x+2g'y+c'=0 \tag{6}$$

where $b', c', d', e', g'$ are constant coefficients normalized with respect to the coefficient of $x^2$. Direct application of HT [3] to the detection of elliptical objects in a digitized picture requires a 5-D array of accumulator; the array is indexed by 5 parameters specifying location (co-ordinates of center), shape and orientation of an ellipse.

More on dimension of circular and elliptical HT has been presented in Section 4.2.2.

### 2.3. HT kernel

HT can be formulated as the integral of a function [71] that represents the data points with respect to a kernel function. This kernel function has dual interpretations as a template in the feature space and as a point spread function in the parameter space: $H(\boldsymbol{\Omega})=\int p(\mathbf{X},\boldsymbol{\Omega})I(\mathbf{X})\,d\mathbf{X}$ where $H(\boldsymbol{\Omega})$ is the value of the HT at the point $\boldsymbol{\Omega}$ and the integral is assumed to be over the whole feature space. The function $p(\mathbf{X},\boldsymbol{\Omega})$ is the HT kernel that determines the particular HT being implemented and is defined jointly on the feature space and parameter space. $I(\mathbf{X})$ is the function that represents the feature set. In discrete HT implementation we have $H(\boldsymbol{\Omega})=\sum_i p(\mathbf{X}_i,\boldsymbol{\Omega})$ where $\mathbf{X}_i=[x_{1i},..x_{Ni}]$ are feature points defined in an $N$-D feature space and $\boldsymbol{\Omega}=[a_1,..a_n]$ defines a point in the $n$-D parameter space.

Princen [83] shows that the SHT can be considerably improved if the vote of a pixel for a given line depends, in a continuous way, upon the distance of the pixel from the line and becomes zero when that distance exceeds a certain threshold. Since they did not consider line orientations, the kernel of this variant of HT (1-D kernel HT) is a ridge of unit height over orientations, falling smoothly to zero at some finite separation value. It is particularly good at distinguishing between lines. Palmer et al. [72] improved

Please cite this article as: P. Mukhopadhyay, B.B. Chaudhuri, A survey of Hough Transform, Pattern Recognition (2014), http://dx.doi.org/10.1016/j.patcog.2014.08.027

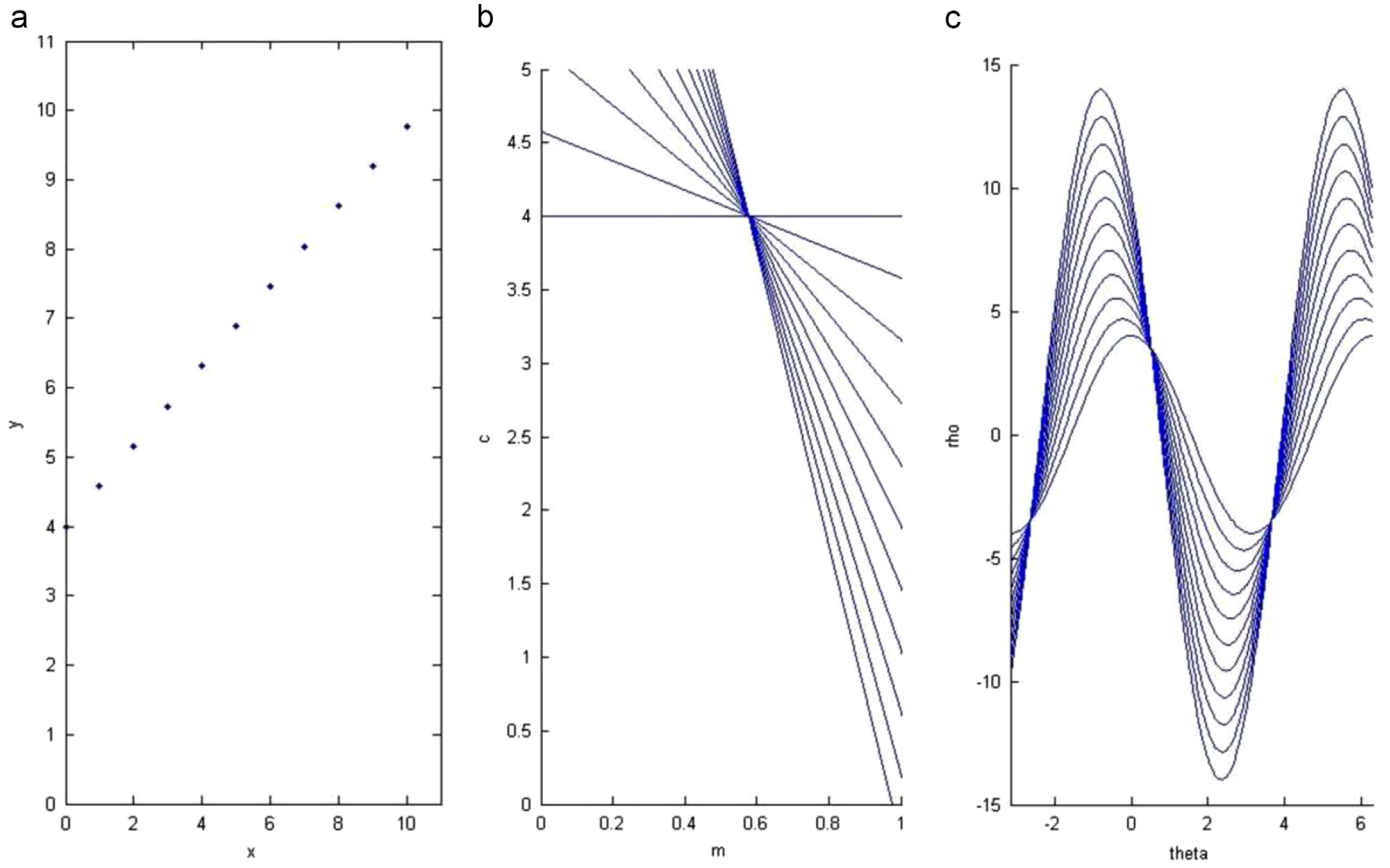


**Fig. 2.** (a) A set of collinear points in image plane; (b) concurrent straight lines in parameter space when slope-intercept parameterization is used; (c) set of sinusoidal curves in parameter plane after $\rho$–$\theta$ parameterization is used.

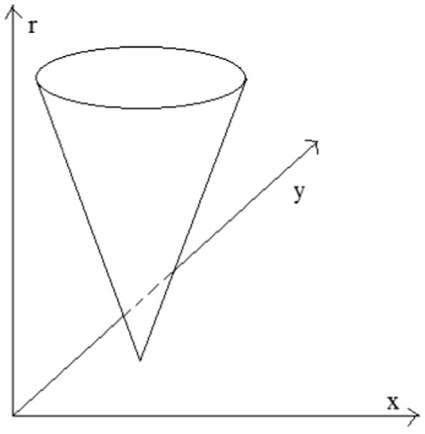


**Fig. 3.** Each pixel of a circle is transformed to a cone in the 3D parameter space.

upon this method and introduced 2-D voting kernels which depend both on the distance of the pixel from the hypothesized line, and on the difference in orientation between the edge pixel (as determined by the edge detector) and the hypothesized line. This helps us to separate closely parallel lines, while keeping interference effects small. An unsupervised statistical kernel modeling of the HT has been proposed in [184], where the resulting estimate is continuous and includes as much information as possible. However, it is more expensive because all image pixels are used (instead of only the edges) and the tails of the kernels are also needed in computing the estimates.

### 2.4. HT as template matched filter

The equivalence of HT and matched filtering technique has been shown by many authors [5,34]. In the generalized HT [9] (see Section 3.1) the shape is represented by a list of boundary points (template) and is an instance of boundaries for the same shape class. Other examples of this class, i.e. other templates can be generated by translating, rotating or scaling on the basic list (Fig. 4).

The difference between template matching and HT is that the former is carried out entirely in the image domain. In most cases a corresponding image point does not exist and the effort in calculating this template point is irrelevant to calculating the degree of match between model and image. In contrast, HT always assumes a match between given basic template point and a selected image point and then calculates the transformation parameters which connect them.

Pao et al. [73] introduced the scalable translation invariant rotation-to-shifting (STIS) signature where rotation in image space corresponds to circular shifting of the signature space. Matching in this signature space only involves computing a 1-D correlation of the reference template with the test template.

### 2.5. Relation between Radon Transform and straight line HT

It can be shown [10] that HT is a special case of Radon Transform [84,26,102,168].

The $n$-dimensional Radon Transform $R$ maps a function on $\mathbb{R}^n$ into the set of its integrals over the hyperplanes of $\mathbb{R}^n$. If $\theta \in S^{n-1}$ and $s \in \mathbb{R}^1$ then $Rf(\theta, s)$ is the integral of $f$ over the hyperplane

Please cite this article as: P. Mukhopadhyay, B.B. Chaudhuri, A survey of Hough Transform, Pattern Recognition (2014), http://dx.doi.org/10.1016/j.patcog.2014.08.027

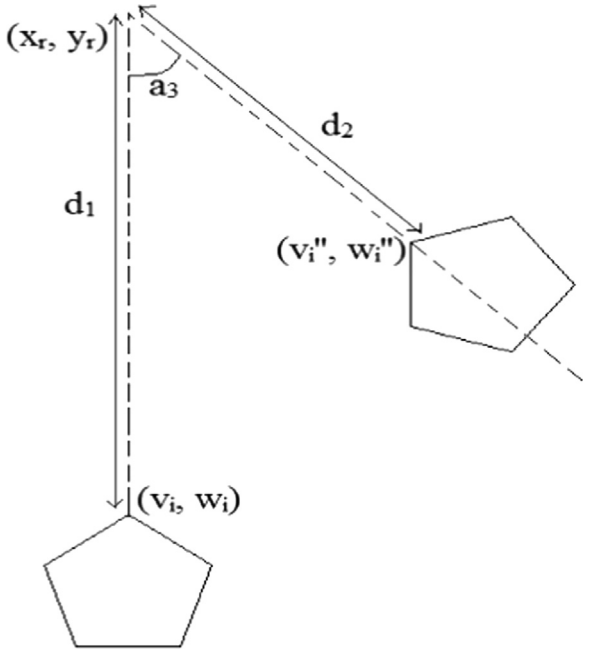


**Fig. 4.** Rotation and translation of a template.

perpendicular to $\theta$ with (signed) distance $s$ from the origin:

$$Rf(\theta,s)=\int_{X.\theta=s} f(x)\,dx=\int_{\theta^{\perp}} f(s\theta+y)\,dx \tag{7}$$

Though Radon Transform can be defined over spaces of arbitrary dimensions, to understand how it relates to HT, it is sufficient to consider the special case of two-dimensional Euclidean plane. If $f(x,y)$ is a continuous two-dimensional function then the Radon Transform is found by integrating values of $f$ along slanted lines:

$$Rf=g(m,c)=\int_{-\infty}^{+\infty}\int_{-\infty}^{+\infty} f(x,y)\delta(y-mx-c)\,dx\,dy \tag{8}$$

where $\delta$ is the Dirac delta function.

According to Eq. (8) the parameter space should be updated with a vote that is proportional to the function value $f(x,y)$. Thus viewing in this way, HT can be regarded as a special case of the Radon Transform in the continuous form. The $(m,c)$ formulation can be written also as $(\rho,\theta)$ formulation:

$$Rf=g(\rho,\theta)=\int_{-\infty}^{+\infty}\int_{-\infty}^{+\infty} f(x,y)\delta(\rho-x\ \cos\ \theta-y\ \sin\ \theta)\,dx\,dy \tag{9}$$

Though equivalent in the continuous form, it has been demonstrated in [102] that HT differs from Radon Transform considerably in the discrete form. HT in most cases is used in the discrete form. In the $(m,c)$ parameterization scheme discrete HT can be defined by suitable choice of sampling intervals such that it gives the same discrete parameter space as found with the nearest neighbor approximation of the discrete Radon Transform. But for the $(\rho,\theta)$ parameterization scheme this cannot be done.

HT can also be viewed as a subtask of Radon Transform inversion. The Radon Transform defined in (8) over two-dimensional Euclidean plane has an exact and linear inverse. The inverse transform maps points in $(\rho,\theta)$ space to straight lines in the original $f(x,y)$ image space. It is given by [161]

$$f(x,y)=Cg(\rho,\theta)=\int_0^{\pi} z[x\ \cos\ \theta+y\ \sin\ \theta,\theta]\,d\theta \tag{10}$$

$$z(\rho,\theta)\triangleq\int_{-\infty}^{+\infty}|\omega|X(\omega,\theta)e^{j2\pi\omega t}\,d\omega \tag{11}$$

where $X(\omega,\theta)$ is the one-dimensional Fourier transform (with respect to $\rho$ co-ordinate) of $g(\rho,\theta)$ at a fixed angle $\theta$ and $C=R^{-1}$ is the inverse Radon operator.

For most practical purposes, a discrete form of Eq. (10) is used. In this case, a sampled parameter space $\mathbf{u}$ is related to image data $\mathbf{v}$ through the equation

$$\mathbf{v}=D\mathbf{u} \tag{12}$$

where the discrete operator $D$, representing the inverse Radon Transform or filter-backprojection operation, is found by discretizing equations (10) and (11). HT can be viewed as reconstructing $\mathbf{u}$ from data $\mathbf{v}$, given the inverse Radon Transform relation (12). The advantage of this inverse problem perspective is that it allows the incorporation of prior information directly into the estimation of the Hough parameter space $\mathbf{u}$.

The Radon Transform is usually treated in the *reading paradigm* [146], where how a data point in the destination space is obtained from the data in the source space is considered. That is, here a shape in the image is transformed into a single pixel in the parameter space. On the contrary, HT is treated in the *writing paradigm*, where it is considered how a data point in the source space maps onto data points in the destination space. Thus HT maps individual pixels in the image space into a shape in the parameter space.

The relation between HT and Radon Transform has inspired several modified algorithms [85,140,161] for shape detection.

## 3. Some major variants

In spite of the robustness of SHT [1,3] to discontinuity or missing data on the curve, its use is limited by a number of drawbacks. (a) The computation time and memory requirements grow exponentially with the number of curve parameters because $n$ parameters, each resolved into $m$ quantized intervals (bins), require an $n$-D accumulator of $m^n$ elements. (b) For high accuracy of localization, finer parameter quantization is required, that entails higher processing time and memory requirements. There is no clear-cut way to optimize the trade-off between accuracy and computation cost for a particular image. (c) A uniform quantization of the parameter space means a non-uniform precision in detecting the curve in the image space. (d) Due to various sources of error, votes in the vicinity of the true parameter vector will increase, leading to peak spreading, which hampers precise detection of maxima in the accumulator. (e) For the detection of each new feature, a separate transformation process has to be initiated. (f) Irrespective of noise, voting contribution of each pixel in the parameter bins is exactly the same (blind voting), resulting in reduction of detection accuracy. (g) SHT cannot automatically detect the end points of line segments.

To overcome these limitations, modifications have been made in one or more stages. Some of these algorithms have introduced features that are significantly distinct from the SHT. In this section we categorize some of these major variants of HT.

### 3.1. Generalized Hough Transform (GHT)

The two-phase learning-and-recognition process, Generalized HT (GHT), introduced by Ballard [9] is the generalization of SHT to detect non-parametric curves. In the learning phase of GHT a model object is used to construct an R-table. A polar co-ordinate system is established in the model object by fixing a reference point and using it as the origin the R-table records the position of all boundary points by their polar co-ordinate values. The rows of the table are indexed by the gradient directions of the edge points on the boundary. During the object recognition or detection phase,

Please cite this article as: P. Mukhopadhyay, B.B. Chaudhuri, A survey of Hough Transform, Pattern Recognition (2014), http://dx.doi.org/10.1016/j.patcog.2014.08.027

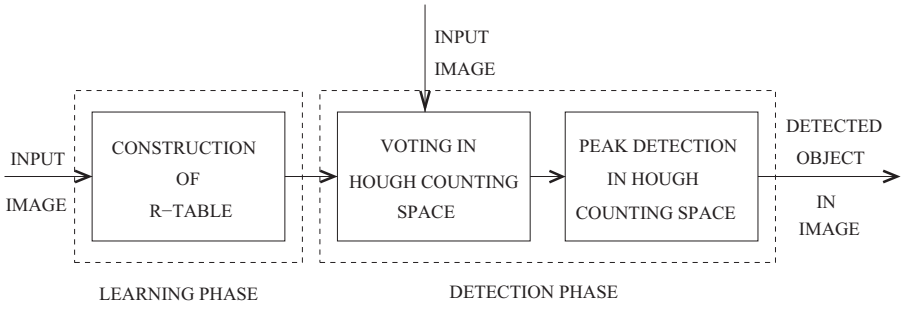


**Fig. 5.** Block diagram of GHT.

a 2D array can be used as an accumulator, called the Hough Counting Space (HCS) or parameter space. Edge points will cast votes to the hypothetical reference point in the HCS according to their gradient directions and the corresponding R-table entries. If the object in the image is identical to the model, then the cell in the accumulator array that corresponds to the reference point will obtain the highest number of votes. The peak value would be equal to the number of boundary points of the object when the model and the object match perfectly.

An initial approach towards a generalized version was made by Merlin and Farber [4] where it was assumed that the target object was the result of translation of the model object but in [9] the idea was extended by including rotations, scale changes. Also local information of object edge points like direction along with position was incorporated. This made the algorithm faster and more accurate. To get stronger constraints for matches, local properties have been extended in [19] to include contrast, position and curvature of contour points. The Dynamic GHT (DGHT) due to Leavers [54] optimizes the computation by using information available in the relative distribution of feature points.

GHT retains the robustness of SHT but cannot detect end points of line segments and require a large number of elements for parallel processing. Further, (a) if the orientation and scale of a new shape is unknown in advance, brute force is usually employed to enumerate all possible orientations and scales for the input shape in the GHT process, thus increasing the number of parameters. As a result, arbitrary shape extraction under similarity or affine transformation leads irremediably to 4D (similarity) or 6D (affine) accumulator spaces, and $O(n^4)$ or $O(n^6)$ complexity algorithms, making the idea impractical. (b) Though the GHT is quite robust for detecting a large class of rigid objects, it cannot adequately handle shapes that are more flexible, i.e. different instances of the same shape are similar, but not identical, e.g. flowers and leaves. (c) In the real world, most objects are perspectively transformed when imaged. The conventional GHT cannot detect perspectively transformed planar shapes.

To reduce the dimensionality of parameter space, researchers have taken recourse to multi-stage voting. For example, in the two-stage GHT by Tsai [108] each boundary point in the image is described by three features namely concavity, radius and normal direction of the curve segment in the neighborhood of the point. The first stage of the voting process determines the rotation angle of the object w.r.t the model by matching the points having the same concavity and radii. The second stage then determines the centroid of the sensory object by matching those points having the same radii, concavity and rotational angles. The affine GHT in [139] positively utilizes pair-wise parallel tangents and basic properties of an affine transformation. After an initial 2-D HT to obtain candidate positions of a target shape, at the second stage a 4-D HT is applied to obtain the remaining four parameters. Since a 4-D parameter space is searched in the second stage, the Adaptive HT [29] is adopted to improve the processing efficiency. A double increment process (Scale and Orientation Invariant GHT (SOIGHT)) has been used in [61], where the accumulator array stores scale and orientation pairs for the points.

For recognition of articulated objects (consisting of rigid parts connected by joints allowing relative motion of neighboring parts), the GHT voting paradigm has been extended in [59] by introducing a new indexing scheme which exploits reference frames located at joints. For natural shape recognition, a supervised HT for Natural Shapes (HNS) has been proposed in [107], where instead of updating the vote at a single point in the accumulator, the GHT has been modified to update for all points that fall on a line segment. This method has been extended in [136] to situations where only one object of the class is available as reference. Two variants of the method based on (a) Binary Mathematical Morphology (BMM) and (b) Gray-Level Mathematical Morphology (GLMM) were suggested in [136].

Olson [123] has analyzed the improvements in accuracy and efficiency that can be gained through the use of imperfect perceptual grouping techniques. Perspective-Transformation-Invariant GHT (PTIGHT) has been proposed in [105], where a Perspective-Reference (PR) table, that contains all perspective transformation information of the template shape, is constructed.

### 3.2. Probability based HT

Several authors have developed approaches of speeding up HT by choosing a subset of data points so that the accuracy of curve detection is reduced by a very small amount. Two such popular algorithms are Probabilistic HT (PHT) and Randomized HT (RHT).

#### 3.2.1. Probabilistic Hough Transform (PHT)

In line detection by SHT [3], for an $N \times N$ image with $M$ object pixels and the $(\rho, \theta)$ plane divided into $N_\rho \times N_\theta$ rectangular bins, the incrementation phase takes $O(M \cdot N_\theta)$ operations and the peak searching phase takes $O(N_\rho \cdot N_\theta)$ operations. In typical applications $M$ is a magnitude higher than $N_\rho$ or $N_\theta$, hence incrementation (voting) stage dominates the execution time. One approach of reducing the complexity of the algorithm is to replace the full-scale voting in the incrementation stage by a limited pool of $m(< M)$ randomly selected object pixels. This class of HT algorithms is referred to as Probabilistic HT (PHT).

The voting phase complexity is now significantly reduced to $O(m \cdot N_\theta)$. Kiryati et al. [63] showed analytically and experimentally that it creates little impairments, even in the presence of distracting features, significant noise and other errors. The optimal choice of $m$ and the resulting computational savings are application dependent.

It is intuitively obvious that for long lines only a small fraction of its supporting points have to vote before the corresponding accumulator bin reaches a count that is non-accidental. For shorter lines a much higher proportion of supporting points must vote. For

lines with support size close to counts due to noise, a full transform must be performed. An adaptive form called Progressive PHT (PPHT), where this is achieved by dynamically controlling the line acceptance threshold (derived theoretically) as a function of total number of votes cast is presented in [120]. In [127] gradient information has been used to control the voting process, thus improving the performance of PPHT. Though PPHT is capable of dealing with multiple curves, it can admit false positives and miss signals.

### 3.2.2. Randomized HT (RHT)

The SHT and PHT are divergent one-to-many mapping, that is, a single pixel can contribute to many $(\rho, \theta)$ values in the parameter space. Another popular probabilistic algorithm, the Randomized HT (RHT) proposed by Xu et al. [56,190], also uses a subset $m$ of $M$ object pixels, but it is a convergent many-to-one mapping. Two randomly selected pixels are used to define a straight line. Here convergent and divergent are used in the sense of many-to-one and one-to-many mapping respectively. For a curve with $n$ parameters, $n$ points are selected at random to calculate the $n$ parameter values of a specific curve. A dynamic accumulator containing a real valued vector and an integer vote value is maintained. For a calculated set of parameters, if it matches an existing set within a tolerance value, the vote is incremented by one; else a new set of values is added with vote 1. In the end, accumulators with votes above the threshold are candidates for detected curves. Since no discretization is performed in the parameter space, high resolution is obtained.

In a theoretical framework, Kiryati et al. [125] have shown that RHT is faster than PHT in high quality images but PHT is more robust than RHT in images contaminated by noise and errors. A brief overview on the developments and applications of RHT for detecting shapes, curves and object motion is given in [190]. The convergent mapping can be altered by varying either the way of getting samples or the way of computing value of set of $n$ parameters, or both. Relying on random points often increase unimportant samples. Instead samples can be obtained by searching a candidate solution via local connectivity and neighbor-orientation [88,124,104], applying relation between line points and chain code direction [193] or by using a priori information about curves [145]. Instead of solving joint equations [175], a solution can also be obtained by least square fitting [156], an $L_p$ norm fitting, or by maximum likelihood estimation.

For a non-linear curve like circle or ellipse arbitrary $n$ points may not uniquely define an $n$-D curve. To detect ellipses in this probabilistic framework, McLaughlin [99] selects three points at a time. Estimates of the tangents to the (possible) ellipse at these points are then calculated and used to interpolate the center of the ellipse. Given the location of the ellipse center the remaining parameters are easily determined. Due to the fact that usually more "virtual" ellipses are detected for one "real" ellipse, a data clustering scheme is used in [154]. The algorithm in [190] detects line segments in an edge image and selects every pair of them to test whether they pertain to the same ellipse. If they pass the test, they are merged. For the detection of incomplete ellipses in images with strong noise, the Iterative RHT (IRHT) developed in [180] "zooms in" on the target curve by iterative parameter adjustments and reciprocating use of the image and parameter spaces. During the iteration, noise pixels are gradually excluded from the region of interest, and the estimate becomes progressively close to the target.

For circle detection, Guo et al. [164] proposed an adaptive RHT where the parameters are detected adaptively through a moving window. RHT is relatively difficult for multi-circle detection because random sampling leads to considerable invalid accumulation. To improve this target distribution is specified and the sampled parameters are weighted in [141]. Li and Xie [142] analyzed the error propagation and sampled the points that were most likely to be located on the circle. Jiang [217] used probability sampling and optimized methods for determining sample points and finding candidate circles, improving sampling validity and preventing false detections. Based on a parameter-free approach without using any accumulator arrays, the RCD method proposed in [126] first randomly samples four edge pixels of which three pixels are used to construct a possible circle, and the remaining one is used to confirm whether it can be promoted to a candidate circle or not. A multi-evidence-based sampling strategy which used three evidences to discard a large number of invalid possible circles is presented in [214].

### 3.2.3. Other probabilistic approaches

Another probabilistic approach (Monte Carlo HT) was suggested in [58] using Monte Carlo algorithms. They used random sampling partially similar to RHT but the accumulator space is fixed. The probability of failure of this algorithm is within tolerance in most applications.

Although RHT and PHT are computationally very fast, they are prone to noise because the local gradient information is affected by noise or distorted shapes.

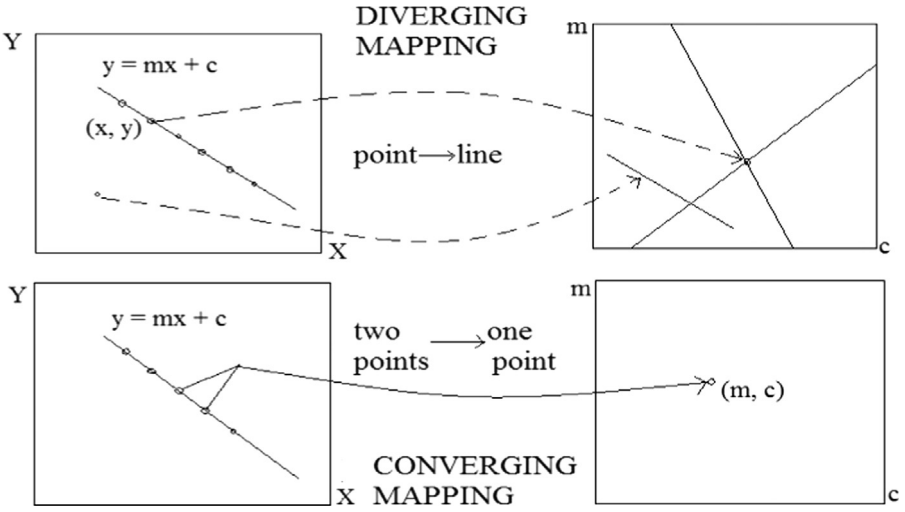


**Fig. 6.** Divergent mapping of SHT vs convergent mapping of RHT [190].

**Table 1**
Comparison of SHT, GHT and RHT [96].

| ALGORITHM | SHT | GHT | RHT |
|---|---|---|---|
| **Image type** | | | |
| Binary | √ | √ | √ |
| Grayscale | × | √ | × |
| **Target** | | | |
| Line | √ | × | √ |
| Circle | √ | √ | √ |
| Parametric | √ | √ | √ |
| Arbitrary | × | √ | × |
| **Speed** | Slow | Slow | Fast |
| **Storage** | High | High | Low |
| **Accuracy** | Medium | Medium | High |
| **Resolution** | low | low | Any |

**Table 2**
Comparison of characteristic features of SHT, PHT and RHT [88].

| Method | Line parameters | Mapping | Accumulator | Sampling | Detection |
|---|---|---|---|---|---|
| SHT | $\rho,\theta$ | One-to-many | 2D array | All points | All lines |
| PHT | $\rho,\theta$ | One-to-many | 2D array | Subset | All lines |
| RHT | $m,c$ | Many-to-one | 2D linked list | Enough | Line by line |

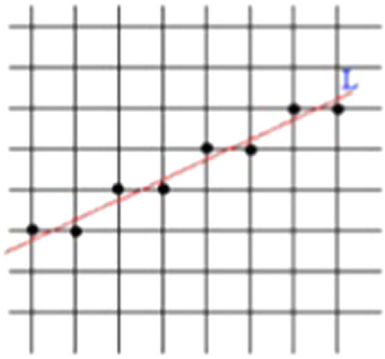

**Fig. 7.** Generation of DSL.

### 3.3. Digital Hough Transform (DHT)

The SHT variants detect straight lines in the analog pre-image. Kiryati et al. [64] refer to them as "Analog HT". These variants do not consider location errors due to image digitization.

The Analytic Hough Transform (AHT) [49] addresses the problem of determining whether a given set of pixels has the digital straight line (DSL) property. A DSL is the result of digitization of a straight line segment. Any digital arc $S$ is a DSL iff it satisfies the chord property [147]. Let $p,q$ be two points of a digital image subset $S$. $\overline{pq}$ is the continuous line joining $p$ and $q$. $\overline{pq}$ lies near $S$ if for every real point $(x,y)$ on $\overline{pq}$, $\exists$ a point $(i,j)$ on $S$ such that $\max\{|i-x|,|j-y|\}<1$. $S$ has the chord property if for every $p,q$ on $S$, the chord $\overline{pq}$ lies near $S$.

AHT [49] employs the slope-intercept parameterization and a non-uniform parameter space quantization scheme, where the $(m,c)$ space is partitioned into four subspaces called the Analytic Hough Region (AHR). If several pixels are collinear with a set of lines, their AHT regions will overlap on a small polygon in one of the four AHRs. Such domains were originally described and characterized in [18]. Lindenbaum et al. [55] proved that the maximum number of possible DSLs in an $N\times N$ digital binary image is $O(N^4)$. Analog HTs, which employ analog equations of straight line, yield approximate solution to the problem of finding DSLs, while the AHT gives exact solutions. The Inverse AHT (IAHT) converts these parameter space polygons into a pair of convex hulls in image space. A real line passes through these hulls iff it passes through every pixel connected with the parameter space polygon. Thus the IAHT generates a pair of simple geometric boundaries in image space that associate pixels with polygonal AHT solution regions.

In [46] the effect of the implicit line quantization on the parameterization of the HT is presented and the sensitivity of the discrete HT line detection has been formulated. The distribution of lines in the natural set determines the precision and reliability with which straight lines can be measured on a discrete imaging array.

Kiryati et al. [64] have compared and analyzed Digital HT (they have mainly considered the Analytic HT [49]) and the conventional, i.e. Analog HTs . Resolution has been defined as the worst case ambiguity in the location of straight lines that intersect opposite sides of the image and set all pixels in between. In the DHT, the resolution and the required number of accumulators are fixed and governed by the dimensions of the digital image, which can only be coarsely modified by decimation. In Analog HT the number of accumulators (and the resulting resolution) can be set by design according to specifications. Also, DHT implicitly assumes that the discretization of the image is the dominant source for edge-point location errors. Thus, in a noisy image or in high resolution applications, Analog HTs score higher.

### 3.4. Fuzzy Hough Transform

The Fuzzy HT, introduced by Han et al. [81], is based on the realization that a shape does not lend itself to a precise definition because of grayness and spatial ambiguities, and therefore can be considered as a fuzzy set. Fuzzy HT detects shapes by approximately fitting the data points to some given parametric shapes. For this purpose, around each point on the perfect shape defined by the parametric form, a small region is defined, and each pixel in this region, i.e. each pixel in the vicinity of the perfect shape contributes to the accumulator space. Thus the accumulator values exhibit a smooth transition from the higher to lower values so that the peaks can be identified unambiguously even for certain distorted image shapes. A theoretical quantification of shape distortion of the Fuzzy HT has been provided in [153].

Bhandarkar [79] presented a fuzzy-probabilistic model of the GHT called Weighted GHT (WGHT) where each match of a scene feature with a model feature is assigned a weight based on the

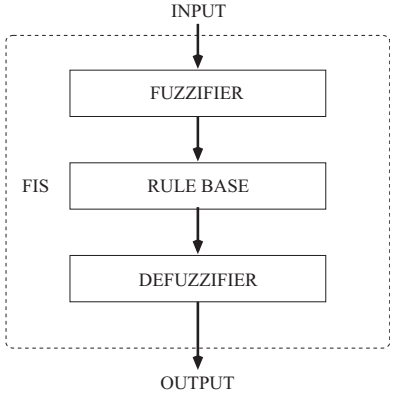


**Fig. 8.** The scheme of a fuzzy inference system (FIS) [189].

**Table 3**
Some major disadvantages of SHT and their popular remedies.

| Disadvantage | Short description | Remedy |
|---|---|---|
| Parametric curve detection | SHT detects curves with an analytic equation. | Using GHT [9] and its variants. |
| Dimensionality | Dimension of parameter space increases with number of parameters and unknown scale and orientation ⇒ More computation. | Divide and conquer approach. |
| Inaccurate parameterization | Results in process noise or model noise. | Suitable parameterization and mapping. |
| Uniform quantization | Results in reduced precision of curve detection. | Sub-unity quantization step for intercept [113],uniform quantization (Diagonal [78], hifi [45], Yuen's [67]), non-uniform quantization [169,181]. |
| Blind voting | Each pixel contributes equally for a feature detection. | Probabilistic vote [129], bandlimiting the parameter plane [62], non-voting approach (Hough-Green Transform) [166], surround suppression [187], voting kernels [114], voting in image space [80]. |
| Peak spreading | A number of cells in the neighborhood of the actual parameter cell gets accumulated. | Proper voting. |
| Line segment and line length detection | SHT can detect straight lines with infinite length and negligible width, while actually they are at least 1 pixel thick and of finite length. | Using additional information like connectivity [206] and degree of vote spread [86], utilizing image and parameter space [160], rotation transform method [65], dual Hough space [162]. |
| Noise and distortion | HT performance degraded by inherent bias of $(\rho,\theta)$ parameter space, statistical noise due to irrelevant structures, background noise, feature distortion. | Suitable parameterization scheme, Iterative RHT [180]. |
| Flexible object and perspectively transformed shape detection | HT cannot detect perspectively transformed and flexible shapes. | HT for Natural Shapes (HNS) [107], Perspective-Transformation-Invariant GHT (PTIGHT) [105], imperfect perceptual grouping technique [123]. |

qualitative attributes assigned to the scene feature. This approach is effective in pruning the search space of possible scene interpretations and also reducing the number of spurious interpretations explored by the GHT. The Fuzzy GHT (FGHT) [189] employs the concept of fuzzy inference system in constructing the R-table, which consists of a set of fuzzy rules which fuzzifies the votes of edge pixels for the possible location of the center.

## 4. Characteristics, limitations and improvements

The characteristics and limitations of HT have been widely studied and many methods have been proposed to improve the performance. We have pointed out some limitations in Sections 2 and 3. Also, some limitations and remedies are presented in Table 3. Here we analyze these limitations in terms of parameterization, mapping, quantization, voting and peak detection. We also throw some light on the remedial measures advocated in the literature.

### 4.1. Parameterization and mapping

A type of noise called “process” or “model” noise arises from inadequate parameterization, sensor distortions and parameter space quantization. By suitable parameterization of the HT, favorable properties like boundedness and discretization and theoretical insights like parameter space geometry can be achieved. A general parameterization based on homogeneous co-ordinates is presented in [51]. It has been shown that the various parameterizations published in the literature can be obtained from this scheme. A description of some of the popular parameterizations is given in Section 2.1.

Most parameter transforms are local in the sense that a small neighborhood operator is used to detect possible instances of a feature in the image data. The local estimates are then combined globally to find the geometric features. But to extract complex features, higher order geometric properties have to be extracted using small neighborhood operators, making the process highly noise-sensitive. Califano et al. [39] introduced generalized neighborhood techniques which exploit the correlated information contained in distant parts of the same image. Unfortunately, the response also becomes more complicated because false features may be detected due to a peculiar form of correlated noise. Another cause of concern is the isotropic nature of SHT in image-parameter mapping. As a remedy the Weighted Polarized HT (WPHT) [37] restricts the mapping in a polarizing zone, eliminating the mappings which are ineffective. In addition, window centroids are transformed instead of the original edge points, leading to a more condensed distribution on Hough space.

### 4.2. Problem of dimensionality

With increasing curve parameters, dimensions of parameter space increase, resulting in an exponential increase in computation. This is further augmented by the process of pixel-wise mapping in HT. To overcome these drawbacks decomposition of parameter space and applying a divide and conquer approach in the image plane (sub-image method) are used.

#### 4.2.1. Sub-image method and divide and conquer approaches

Sub-division of image space has been done by authors like Olson [123], who constrained each sub-problem to consider only those curves that pass through some subset of the edge pixels up to the localization error. Using it for industrial images, Davies [22] was able to locate objects within 1 pixel and orientation within about 1°. In [95] the image is decomposed into rectangular blocks and the contribution of each whole block to the HT space is evaluated, rather than the contribution of each image point. In the Concurrent Modified Algorithm for GHT, the authors [135] subdivided both the target and template images and the allocation of

Please cite this article as: P. Mukhopadhyay, B.B. Chaudhuri, A survey of Hough Transform, Pattern Recognition (2014), http://dx.doi.org/10.1016/j.patcog.2014.08.027

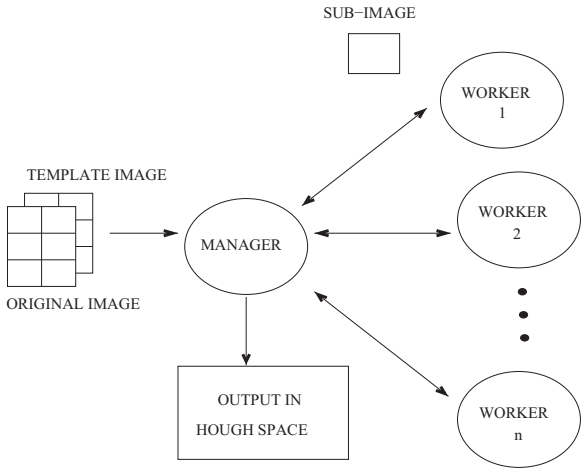


**Fig. 9.** Manager–worker model [135].

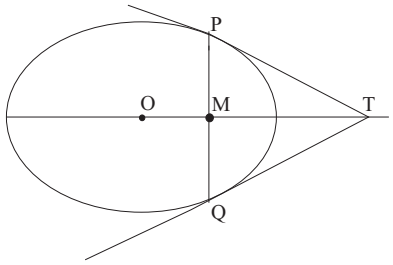


**Fig. 10.** Construction used for ellipse center-finding in [86,104].

sub-images to processors is managed through a variant of the manager/worker technique (Fig. 9).

To avoid pixel-wise processing of each subregion, Ser and Siu [74] evaluated only the shaded pixel with the Sobel operator, while the neighboring 8 pixels are evaluated only if the gradient magnitude of the shaded pixel is greater than a pre-defined threshold. In a different algorithm the authors [91] introduced a Region-Bit-Map (RBM) for each sub-image to identify peaks contributed from a particular region. To overcome redundancies, Chau and Siu [118] determined the characteristic angle that can lead to a number of index entries in the R-table, a small number of entries per index and reduction of the number of spurious assessments of boundary points.

An alternative divide-and-conquer approach is parameter space decomposition. Pao et al [73] have shown that the Straight Line HT (SLHT) of closed smooth curves offers a natural way to decompose the parameter space into three subspaces, namely the translation, rotation and intrinsic space. The curve detection procedure only involves searching the orientation of the curve, the intrinsic curve parameters and translation of the curve can be determined by analyzing the transform space representation. In the Fast HT (FHT) developed by Li et al. [23,24] the parameter space, represented by a $k$-tree, is divided recursively into hypercubes from low to high resolution and HT is performed only on the hypercubes with votes exceeding a certain threshold. A hypercube receives a vote only when a hyperplane intersects it.

The Fuzzy Cell HT (FCHT) [94] iteratively splits the Hough Parameter Space into fuzzy instead of crisp cells which are defined as fuzzy numbers with a membership function of $n$ parameters ($n$=no of curve parameters). After each iteration, the fuzziness of the cells is reduced and the curves are estimated with better accuracy. The uncertainty of the contour location is transferred to the parameter space and helps us to estimate curves with better accuracy than classical HT especially when dealing with noisy images. The RHT is combined with the FCHT (Randomized FCHT (RFCHT)) in [103] to obtain the advantages of both.

#### 4.2.2. *Handling the problem of dimensionality for circles and ellipses*

Most researchers follow a multi-stage divide and conquer strategy in which the parameter space of dimension $N$ is decomposed into several subspaces of respective dimension $n_d$ (generally $\sum n_d = N$) using geometric constraints which define relative position between a set of points. The first stage is usually the center-finding stage and the remaining stages are aimed at finding the remaining parameters of the best fitting ellipse or circle after the candidate points have been selected.

In [15,30] a 2-D array is used in the first stage to determine the mid-points of lines joining two object points with parallel tangent. Then a 1-D array is used for testing candidate points of an ellipse. These points follow the equation

$$x^2 + b'y^2 + 2d'xy + c' = 0, \quad b' - d'^2 > 0 \tag{13}$$

This method of center-detection can be inaccurate for partially occluded ellipses where they do not contain sufficient points that are symmetrical about the center. Wallace [17] estimates the 3 parameters of (13) in two further steps using the following equation obtained after differentiating (13) with respect to $x$:

$$x + b'y(\mathrm{d}y/\mathrm{d}x) + \mathrm{d}'(x(\mathrm{d}y/\mathrm{d}x) + y) = 0 \tag{14}$$

The disadvantage of this approach is that though dimension of accumulator is reduced, a large amount of storage is required. Also, due to decomposition into several steps, the chance of error propagation rises. Tsuji and Matsumoto [8] used a least mean squares method to evaluate all 5 ellipse parameters at a time. The use of least square procedure makes it sensitive to noise. In [186] the image is sub-divided based on convexity of ellipse edge.

In [48] the center of ellipse is found as follows: let P and Q be two points on an ellipse with non-parallel tangents intersecting at T. Let M be the mid-point of PQ. Then the center of the ellipse (O) must lie on TM (Fig. 10). To improve the speed of this method, in [44] ellipse orientation is extracted and then the major and minor radii are found in a 2D accumulator array.

Estimating the parameters based on local geometric properties often suffer from poor consistency and locating accuracy because of noise and quantization error. That is why, the global geometric symmetry of ellipses is used in [103] to reduce the dimension of the parameter space. After locating possible centers of ellipses using a global geometric symmetry, all feature points are partitioned into several subimages according to these centers and then geometric properties are applied in each subimage to find possible sets of three parameters (major and minor axis length and the orientation) for ellipses.

For circle detection, a pair of 2-D accumulator arrays are used in [60]. The first 2-D array represents the $x$ and $y$ co-ordinates of the centers of the predicted circles and those of the second represent the co-ordinate of the center and radius of the predicted circles. The size invariant method in [143] is based on the symmetry of the gradient pair vectors and it can detect circles that are brighter or darker than their backgrounds. In [121] a two-part algorithm is used. The first part is a 2-D bisection based HT that relies on the property that perpendicular bisector of any chord of a circle passes through its center. The second part is a 1-D radius histogramming that validates the existence of these circles and calculates their radii.

Please cite this article as: P. Mukhopadhyay, B.B. Chaudhuri, A survey of Hough Transform, Pattern Recognition (2014), http://dx.doi.org/10.1016/j.patcog.2014.08.027

### 4.3. Quantization issues

A major problem with HT arises from the effects of image quantization, uniform parameter space sampling and discretization, that makes the distribution of parameters non-homogeneous and non-equiprobable [36]. This is aggravated by the presence of sensor noise and optical distortions, resulting in a spread of votes around the actual bin in the parameter space and hence leading to inaccuracy in peak detection.

In [13] it is shown that a decrease of $\Delta\rho$ and $\Delta\theta$ not only reduces the spread but also enhances the effect of image quantization. For digital straight lines formed by concatenation of short horizontal and vertical line segments, Guo and Chutatape [117] have shown that for lines oriented around $\pi/4$ or $3\pi/4$ radian the accumulation result is better. Peak distortion increases for lines around horizontal and vertical directions. However for a precisely horizontal or vertical line, the peak distortion does not occur. Consequently, a new approach called a variable $\Delta\rho$ HT having $\Delta\rho$ as a function of $\theta$ has been proposed. In [92,113] it is shown that a sub-unity quantization step for the intercept is a necessary and sufficient condition for the members of the parameter space to represent subsets of discrete straight lines (DSLs).

Several authors have proposed uniform quantization like the hifi quantization by Risse [45], that gives the coarsest quantization such that no two realizable lines in the image correspond to the same accumulator cell. Yuen and Hlavac [67] suggested that it is meaningless to quantize any variable finer than the uncertainty of the variable. Thus the diagonal quantization technique in [78] defines quantization intervals of the parameter space by considering only the greatest of the $y$ or $x$ component in the back transformation of the HT.

Due to non-uniformity of angle and distance spacing between adjacent straight lines in an image (Fig. 11), a non-uniform quantization is used in [169,181]. Experimental results show that the non-uniform quantization of Hough space improves the accuracy of line segments detection substantially with no efficiency loss.

### 4.4. Clutter in image plane vs cluster in parameter space

Some factors that influence the performance of the HT are (1) number of points in the image plane, (2) size of clusters associated with the sought after curve; (3) spatial distribution of the clusters in the parameter space when both the correct and the incorrect transform are applied. Intensive study on the characteristics of the HT and Hough-like transforms [6,7] showed that points tend to cluster in parameter space (packing) if and only if the corresponding points in image plane lie on the same underlying curve. The transform method works well when the clusters in parameter space are well-separated. Given a transform, if the parameters of the underlying curves are uniformly distributed and the appropriate transform is applied, then the resulting parameter points should again be uniformly distributed. If this does not hold, artificial clusters will appear in parameter space, where a bunching of parameter points will occur. This feature is called "homogeneity".

**Table 4**
Quantization Interval.

| Parameters | Diagonal quantization [78] | Hifi quantization [45] | Yuen's quantization [67] |
|---|---|---|---|
| $\rho,\theta$ | $\Delta_d\rho = 1/2\sqrt{2}$<br>$\Delta_d\theta = 1/2N$ | $\Delta_h\rho = 1/N(N-1)^2$<br>$\Delta_h\theta = 1/2(N-1)^2$ | $\Delta_y\rho = 1$<br>$\Delta_y\theta = 2/N$ |
| $m,c$ | $\Delta_d m = 1/N$<br>$\Delta_d c = 1$ | $\Delta_h m = 1/N(N-1)$<br>$\Delta_h c = 1/N(N-1)(N-2)$ | Not defined |
| $\gamma,c$ | $\Delta_d\gamma = 1/2N$<br>$\Delta_d c = 1$ | $\Delta_h\gamma = 1/2(N-1)^2$<br>$\Delta_h c = 1/(N-1)(N-2)$ | Not defined |

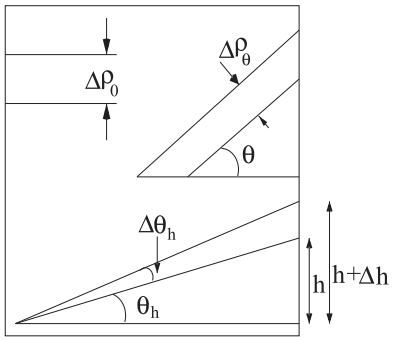


**Fig. 11.** Non-uniformity of angle and distance spacing between adjacent straight lines.

### 4.5. Accumulation or voting and peak detection

It has already been shown in Section 2.5 that the classical Radon transform on the two dimensional Euclidean plane transforms a function $f$ into a function $g$ defined on the set of all straight lines of the plane. The domain of $g$, that is the set of all straight lines, is the *accumulator* [76]. The topological structure of this space is such that the graph $K_{3,3}$ can be embedded into it and hence by Kuratowski theorem the accumulator cannot be embedded into the plane. This poses a major problem in the accumulation phase.

Another reason for the inaccuracy of HT is the "blind" nature of voting phase where each object pixel contributes one vote. This approach helps us to handle line discontinuities but is a major source of inaccuracy because each pixel may carry different uncertainties. It is shown in [6,7] that the popular accumulator method implies sampling of a non-bandlimited signal. The resulting aliasing accounts for several familiar difficulties in the algorithm. Bandlimiting the parameter plane would allow Nyquist sampling, thus aliasing could be avoided. A non-voting alternative, the Hough–Green Transform (HGT) is suggested in [166], whose accuracy is close to HT and has other advantages like non-occurrence of offset dependence and/or vote-splitting artifacts and near perfect isotropy.

For voting, Guo and Chutatape [119] considered only candidate patterns that cross at least two feature points, so that much of the unnecessary computation can be avoided. This method is combined with the Windowed RHT in [195] employing many-to-one mapping and sliding window neighborhood technique to alleviate the computational and storage load. The high-resolution parameter space requirement for high accuracy has the disadvantage that votes will be sparsely distributed in parameter space and therefore a reliable means of clustering them is needed. This leads to multi-resolution schemes that use reduced information content of multi-resolution images and parameter arrays at different iterations. For example, the iterative coarse-to-fine search strategy (Adaptive HT) of [29] used a small accumulator array which is thresholded and then analyzed by a connected components algorithm which determine the parameter limits used in the next iteration. This method, however, produces spurious peaks at coarse resolution when applied to complex images. A Fast Adaptive HT (FAHT) is developed in [42] where at each resolution a strategy is employed to analyze the parameter space so that more appropriate parameter limits for subsequent processing can be defined. A logarithmic range reduction for faster convergence is proposed in [68]. A two-phase adaptive method is proposed in

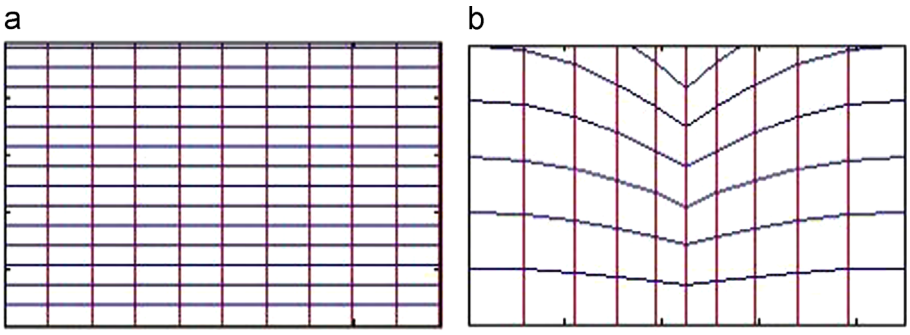


**Fig. 12.** Shape of bins for (a) uniform quantization and (b) non-uniform quantization of parameter space.

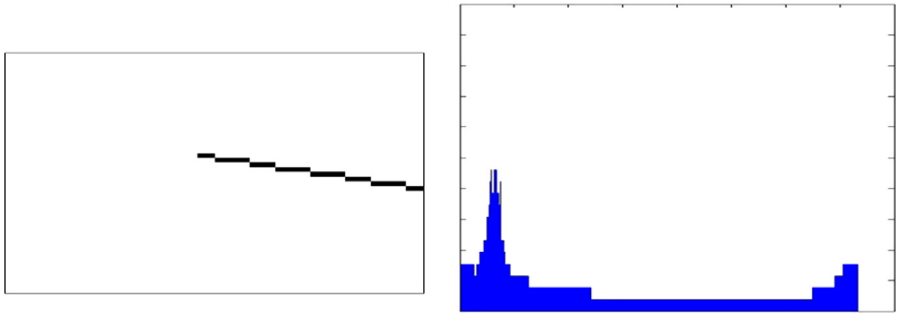

**Fig. 13.** Peak spread corresponding to a straight line segment (left).

[163] where the authors applied a criterion derived from the observed stability of the peak position in the parameter space to stop the transform calculation.

Voting kernels and voting weights have been used to take care of pixel uncertainties towards object detection. The kernel designed in [114] depends on appropriate shape descriptors of the connected regions while [187] introduced an efficient measure of isotropic surround suppression.

Toronto et al. [174] proved that HT is implicitly a *Bayesian process* – given some feature points it computes an unnormalized posterior distribution over the parameters of a single shape. The probabilistic scheme in [129] analytically estimates the uncertainty of the line parameters derived from each feature point, based on which a Bayesian accumulator updating scheme is used to compute the contribution of the point to the accumulator. The error propagation technique for uncertainty computation of this paper was improved by Bonci et al. [152] by the characterization of the covariance matrix and inference of joint probability by the normal joint distribution.

Chang and Hashimoto [80] made the voting process on the image space rather than normal parameter space, then converted the peak detection in the parameter space into a parameter optimization problem. Since large memory for the discrete parameter space is not needed, it requires much lower storage and execution time than the conventional HT.

### 4.6. Line segment, line length detection and influence of line thickness on detection

Line segments are much more meaningful in feature extraction because they form the boundary of objects like buildings, fields, and box. Improving the accuracy of line segment detection may reduce the complexity of subsequent high-level processing, common in cartographic feature detection algorithms.

The algorithm STRAIGHT (Segment exTRAction by connectivity-enforcInG HT) [205] extracts long connected segments by incorporating connectivity in the voting procedure by only accounting for the contributions of edge points lying in increasingly larger neighborhoods. Yang et al. [111] use a weighting scheme based on the likelihood ratio test statistics to detect short, thick and connected line segments. Ioannou [86] has used information like amount of spread of votes in the accumulator.

In the rotation transform method of [65] the edge image is rotated about the center of the image plane by a fixed angle step, and in each rotated image, search is carried out in the horizontal and vertical directions to find the end points of horizontal and vertical line segments. Cha et al. [162] split the Hough space into two linear sub-spaces, simplifying the search algorithms. Augmenting the dual space HT with a 3rd parameter (the $x$- or the $y$-axis of image space) helps us to determine the length of line segments.

According to Song and Lyu [160] limitations of most variants of HT to detect line thickness in large images like engineering drawing arise because they only work on the HT parameter space. So the method in [160] utilized both the parameter space and the image space.

### 4.7. Noise and distortion

Analyses show that the presence of a large number of noise edge pixels, unimportant image structures or textual-like regions greatly contribute to the deterioration of the performance.

Brown [14] analyzed HT behavior in various forms of noise and concluded that the $(\rho,\theta)$ parameter space has inherent bias. Real point spread functions have a central peak and non-zero side-lobes that contribute to bias. This bias has been treated as the appearance of white noise in the image space by Maitre [25]. Wada and Matsuyama [75] first showed that the bias is caused by the uniform quantization of the parameter space. To eliminate the bias, a new parameter $\gamma$ representing a non-uniform quantization along the $\rho$-axis is introduced and uniform quantization is done on the $\gamma$–$\theta$ parameter space. Hunt et al. [53] have proposed a statistical signal detection theory for curve detection in noisy images. Detection performance is measured using Receiver Operating Characteristics (ROC).

Please cite this article as: P. Mukhopadhyay, B.B. Chaudhuri, A survey of Hough Transform, Pattern Recognition (2014), http://dx.doi.org/10.1016/j.patcog.2014.08.027

Eric et al. [50] concluded that GHT does not scale well for recognition of occluded or noisy objects because of the following reasons. First, the range of transforms specified by a given pair of model and image features can be quite large. Second, the percentage of buckets specified by a single data-model pair increases with increasing sensor uncertainty and reduces (i.e. increase of coarseness of Hough space) with increased occlusion. Third, the number of model-image pairs likely to fall into the same Hough bucket at random can be quite high, resulting in larger random clusters.

The noisy pixels have even more serious impacts on randomized algorithms. Guo et al. [178] proposed a PHT for line detection utilizing surround suppression, which reduces the weight of noisy pixels in complex background or texture-like regions, suppresses the peaks produced by these pixels, and subsequently put emphases on peaks formed mainly by pixels on the boundaries between significantly different objects. The Iterative RHT (IRHT) [180] detects incomplete ellipses in images with strong noise by "zooming in" on the target curve by iterative parameter adjustments and reciprocating the use of image and parameter spaces.

## 5. Implementation issues

The implementation of a method should satisfy the constraints of the applications in terms of time and memory needs. We discuss some implementation issues in this section.

### 5.1. Software solutions

The software solutions for a high-precision, high-dimensional, fast and less space consuming HT range from new data structure to the formulation of a known algorithm in a computer-friendly way.

#### 5.1.1. Data structures

To represent accumulator array O'Rourke [11] used Dynamically Quantized Space (DQS) that allocates resources where they are most needed to detect the parameter space peak. Though a little inefficient in space, the Dynamically Quantized Pyramid (DQP) used in [12] has the advantage of fixed resource allocation and convenient hardware implementation (e.g VLSI). Kim et al. [35] represented an $n$-D parameter space with $m$ discrete values for each parameter by $n$1-D arrays of length $m$ each. Thus space complexity reduces from $m^n$ to $mn$. To construct each AHR for Analytic HT [49], a linked line list instead of polygons is employed in [66]. Also, all floating point computations are replaced by faster, fixed word-size, integer operations because all values may be stored as rational numbers.

#### 5.1.2. Neural network (NN)

To increase speed, implementation of HT with neural networks has been suggested in [43,69,116]. These approaches mainly accept image co-ordinates as the input and learn the parametric forms of the lines adaptively.

#### 5.1.3. Other computer-friendly algorithms

Shapiro [6] and Satzoda et al. [182] proposed parallel implementation by dividing the picture plane in small areas and processing each area in parallel. The parallel guessing principle of [28] computes the HT incrementally and terminates computation when a significant parameter peak is identified. The gradient based HT in [98] avoids the use of a large 2-D Hough Space and can be implemented in parallel. By keeping transformed data packed closely together in lists and accessing only small, 1-D data structures, memory requirements are significantly reduced.

Pavel and Akl [101] examine the possibility of implementing the HT for line and circle detection in an $N \times N$ image on Arrays with Reconfigurable Optical Buses (AROBs) in a constant number of steps. An Integer HT (IHT) which allows efficient integer operations only is proposed in [85]. Olmo and Magli [132] have shown that IHT is 2–3.5 times faster than the HT since floating point operations are avoided.

### 5.2. Hardware solutions

There can be more than one approach to achieve real-time implementation. In this paper we mainly discuss about parallel processing, one of the most popular among these.

#### 5.2.1. Parallel implementation among processing elements

There are various configurations for parallel implementation of HT [110,38], differing in the way the image and the transform spaces are distributed among the processing elements (PEs). In *Global image memory and distributed transform memory* all PEs have access to all image pixel points with each computing the HT for a different segment of the transform space. In contrast, in *Distributed image memory and global transform memory*, each PE has access to a different segment of the pixels in the image but computes the HT for the entire transform space. Finally in *Distributed image memory and distributed transform memory* each PE has access to the image and to a segment of the transform space.

The parallel implementation scheme of Merlin and Farber [4] had the advantage that the same system can do other tasks like edge detection or thinning. The drawback lies in the speed, to compensate for which the number of processing elements can be increased, making a large and expensive system. Efficient parallel image processing pipeline architecture has been used in [27,33].

The SIMD (Single Instruction Multiple Data) consists of square arrays of simple processing elements (PEs) which can communicate with 4 or 8 neighbors. In this parallel architecture all PEs concurrently execute the same instructions on different items of data. The mapping of HT onto these architectures was first considered by both Silberberg [21] and Li [23,24]. In [21] each PE is assigned both an image feature and a cell of parameter space while in [23,24] each PE is assigned an image feature and the co-ordinates of a parameter cell are broadcast simultaneously to every PE by a central controller. These steps speed up the HT by a factor of $O(n)$. However, the votes have to be routed to their correct places in the accumulator and on a simple 2-D square mesh with only local shifting operations, which requires $O(\sqrt{n})$ steps.

The SLAP (Scan Line Array Processor) [41], a system having a linear array of SIMD vector processors, assigns a single PE to each column of the image and the array moves over the image and processes all pixels of a row concurrently. Some SIMD instructions were proposed in [179] to speedup the calculation of HT specific elementary functions using a specialized look-up table. A Multiple SIMD (MIMD) array was used in [52] where tasks of calculating the accumulator array and finding the peaks are performed together.

#### 5.2.2. Dedicated hardware and VLSI implementation

The HT processor can be implemented in real-time on different bases like application oriented VLSI components or special purpose component like Histogram/Hough Transform Processor [32] (the earliest commercial hardware implementation of HT).

Most Hough-based methods encounter the evaluation of implicit trigonometric and transcendental functions. This makes the

Please cite this article as: P. Mukhopadhyay, B.B. Chaudhuri, A survey of Hough Transform, Pattern Recognition (2014), http://dx.doi.org/10.1016/j.patcog.2014.08.027

monolithic implementation of the entire algorithm very complex. To overcome this problem, the Co-Ordinate Rotation Digital Computer (CORDIC) based architectures [47,93] were used to generate the vote address in parameter space. Also, a CORDIC-based asynchronous HT architecture suitable for VLSI implementation was proposed in [131].

Lin and Jain [82] proposed a multi-chip-module (MCM) construction which can be configured to have eight HOUGH modules. Systolic arrays consisting of time-delay processing elements and adders can be used to reduce $n$-D feature space to 2-D. Epstein et al. [138] presented the application-specific integrated circuit (ASIC) implementation of the HT as a systolic array for real-time recognition of curved tracks in multi-wire drift chambers.

A real-time Content Addressable Memory (CAM)-based HT algorithm is proposed in [100] where both voting and peak extraction are directly executed by CAM. The CAM acts as a PE array that performs highly parallel processing tasks for the HT and also acts as a memory for 2-D Hough space. Strzodka et al. [144] have employed an inexpensive, consumer-market graphics card as the parallel processing system for GHT. From known object geometry, their hardware accelerated GHT algorithm is capable of detecting an object's 3-D pose, scale and position in the image within less than 1 min. Ito et al. [209] used GPUs (Graphics Processing Unit) for up to 4 times faster ellipse detection.

Field Programmable Gate Arrays (FPGA) have high specificity of an ASIC. But since they target smaller markets they require much less development time while avoiding the development costs, design risks and inflexibility of a custom solution. They are also faster than general purpose processors and high throughput is more often achieved by exploiting the parallelism of the architecture than by operating it at higher clock frequency.

Mayasandra et al. [158] used FPGAs and proposed a Distributed Arithmetic (DA) approach to the SHT. Its use completely eliminates the need for multipliers, by modifications at the bit serial level. Tagzout et al. [134] combined an incremental method with the usual HT to overcome space requirements of FPGA. In [215] both pixel-level and angle-level parallelism have been exploited to reduce resources. Parallel PEs can be used to compute different $\theta$ in parallel. For a given $\theta$, if $p_1=(x,y)$ and $p_2=(x+\mathrm{d}x,y+\mathrm{d}y)$ are two points in the image, then $\rho_2$ corresponding to $p_2$ is related to $\rho_1$ corresponding to $p_1$ as

$$\rho_2=\rho_1+\mathrm{d}x\ \cos\ \theta+\mathrm{d}y\ \sin\ \theta$$

This offset relation is made use of in the pixel-level parallelism. Thus dividing the image into blocks, the $\rho$ value of all neighboring pixels of a central pixel can be calculated by the above offset relation. Also in [215] non-feature pixels have been avoided by a clever use of run-length encoding.

## 6. Real life applications

HT has found immense practical applications in vision problems like object detection, motion detection, biometric authentication, medical imaging, remote data processing, and robot navigation. In this section we review some of these applications.

### 6.1. 3-D object detection

3-D object description has at least two parts: (a) the internal description of the object itself (with respect to an object-centered frame); and (b) the transformation of the object-centered frame to the viewer-centered (image) frame. Often the former is known beforehand and the task reduces to finding the latter.

Silberberg et al. [20] describe an iterative Hough procedure where initially, a sparse, regular subset of parameters and transformations is evaluated for goodness-of-fit, and then the procedure is repeated by successively subdividing the parameter space near current best estimates of peaks. For object detection in 3D scenes with significant occlusion and clutter, a Hough voting approach is used in [201], while Tong and Kamata [200] used a 3D HT to obtain a spectrum on which 3D features are concentrated on the sphere and employ Hilbert scanning to match the objects globally.

### 6.2. Motion detection

Motion estimation is important in video processing tasks like standards conversion, frame-rate up-conversion, noise reduction, artifact suppression and video compression.

A 2D non-model based motion detection algorithm, called Motion Detection using RHT (MDRHT), suggested in [70], detects the motion of a single object exploiting edge pixels only as feature points. Kalviainen [97] extended it to use both edge pixels and the intensity-gradient vector at edge pixels and generalized it to detect multiple moving objects. For multiple-motion analysis, the essential part is segmentation of independently moving objects. It is determined by Tian and Shah [109] based on a 3D rigidity constraint. The global Hough based evidence gathering technique to extract concurrently the structural and motion parameters of a feature from a temporal sequence of images is reported in [106,130].

Given an unstable video, image stabilization aims at synthesizing a new image sequence such that the unwanted image motion caused by camera motion is removed. Chuang et al. [192] presented a digital image stabilization involving multiple objects motion detection based on block-based HT.

### 6.3. Medical imaging

Automatic object recognition is one of the main tasks in modern medical image (e.g. computer tomography (CT), X-ray radiographs, echocardiographs, and mammograms) analysis problems.

Golemati et al. [155] studied the application of HT to detect diastolic and systolic diameters of the carotid artery. A two-step HT to find an annular approximation of the myocardium in short-axis echo slices is proposed in [219]. A 3-D implementation of GHT to localize the heart [177] and the liver [202] in 3-D CT has been proposed recently. Brummer [57] used 3-D HT for automatic detection of the Longitudinal Fissures (LF) in tomographic scans of the brain. The 3-D vertebra orientation estimation technique in [220] is based on HT to match the projections of the standard 3D primitive with the vertebral contours in biplanar radiographs. Using HT for blood cell segmentation is reported in [207]. Tino et al. [213] formulated a dedicated probabilistic model-based HT to be applied to hexaMplot to detect groups of coexpressed genes in the normal-disease-drug samples.

### 6.4. Biometric authentication

Biometric authentication like finger-print and palm-print matching, and iris detection are done for security purpose.

Fingerprint matching is a difficult task due to large variability in impressions of the same finger. Qi et al. [149] proposed a HT-based fingerprint registration where discretization of the Hough space is not needed under rigid transformation between two fingerprint impressions. To enhance the performance of minutiae based matching in poor quality images, Tong et al. [167] developed a HT-based algorithm where minutiae vectors are established and

Please cite this article as: P. Mukhopadhyay, B.B. Chaudhuri, A survey of Hough Transform, Pattern Recognition (2014), http://dx.doi.org/10.1016/j.patcog.2014.08.027

classified according to vector modules. Ridge features instead of minutiae are used in [157] for fingerprint matching algorithm while in [199] both ridge and minutiae are used to reduce the false matching. For matching smudgy transparent latents Paulino et al. [211] used descriptor-based HT to align fingerprints and measure similarity by considering both minutiae and orientation field information.

Dai et al. [216] studied quantitatively the major features in palm print and used GHT at various steps of their segment based matching and fusion algorithm. A line-based HT is used in [165], which extracts global features for coarse-level filtering in hierarchical palmprint identification system.

A classical way to do iris localization employs edge detection techniques plus a HT to fit a circle for each boundary. Modified HT techniques have been used in many papers like [150,171,183,196]. Jalil et al. [218] present a comparison of techniques namely Circular HT (CHT), Daugman's Integro Differential Operator (DIDO) and Circular Boundary Detector (CBD) for localization of iris region.

### 6.5. Remote sensing

The linear shapes in SAR (Synthetic Aperture Radar) images may correspond to roads, rivers, railways, hedges or forest rides and thus many authors like Cross and Wadge [31] and Tian et al. [212] use HT to extract them. Xu and Jin [176] developed a technique for automatic reconstruction of 3-D building objects, modeled as cuboids, from multiaspect SAR images in one meter resolution.

In a HRR (High Range Resolution) RADAR the size of target is larger than wavelength of the RADAR and RADAR range resolution cells. An approach for noncoherent integration of HRR pulses based on HT has been proposed in [208]. To deal with the scaling of ISAR image and phase wrapping in interferometric ISAR, a cross-range scaling algorithm of interferometric ISAR based on RHT has been proposed in [204].

### 6.6. Robot navigation

Autonomous navigation of robots requires effective and robust self-localization techniques. A probabilistic approach to self-localization that integrates Kalman filtering with map matching based on HT is described in [128]. In [172] the position and the orientation of a mobile robot are estimated from the Hough parameters of several flat surfaces in the environment. Kim et al. [210] used HT for vision based direction determination algorithm of a mobile robot in indoor environment. For automated guidance for agricultural machinery Jiang et al [198] used HT for robust recognition of crop rows. The correlation scan matching method based on matching consecutive readings of Laser Range Finder (LRF) by Graovac et al. [197] uses HT and the Hough spectrum for determining the relative rotation.

### 6.7. Optical Character Recognition (OCR) and document processing

OCR (Optical Character Recognition) is a software tool that has been used to convert image of text from camera, handwritten, scanned or printed materials into say Unicode representation of corresponding characters. Many papers have reported use of HT for character recognition in different scripts like [16] for Hebrew, [151,173] for Arabic, [185] for Persian, [40,89] for Chinese.

An OCR system segments the text image into physical components before performing symbol recognition. A text has a linear structure which can be described, at the symbol level, by a string of characters or words. The physical components corresponding to this linear structure are the lines of text. Thus authors like Likforman-Sulem et al. [90] used HT to detect text lines on hand-written pages which may include either lines oriented in several directions, erasures or annotations between main lines.

Skew angle estimation is also an important component of an OCR and Document Analysis Systems (DAS). HT has been used for this purpose by many researchers [203,206,159]. Ma and Yu [122] consider the lowermost pixels of some selected characters of the text, which may be subject to HT for skew angle detection. Xiangyu et al. [191] proposed a method for aligning lecture slides with lecture videos using a combination of Hough transform, optical flow and Gabor analysis.

## 7. Conclusion

This paper presents a comprehensive and up-to-date survey on various issues of HT which even after 51 years of discovery is a lively topic of research and applications. This is remarkable in technical field where tools become outdated in 5 years. A large amount of work has piled up since the last survey published on HT about 20 years ago. In this paper we have discussed most of them so that the researchers get an overview of the domain and choose the adequate technique for their problem of interest. A list of more than 200 references will help them to know the technique/analysis in detail and guide them to develop their required software. Some packages like MATLAB support conventional HT, but they are not enough for some specialized need.

Apart from its widespread applications in pattern recognition and image processing, there exists scope for further theoretical research on speed, accuracy and resolution of shape detection especially for partial, perspectively distorted and complex curves in 2-D and 3-D. It is hoped that this survey will simulate further interest in attacking such problems.

## Conflict of interest

None declared.

## Acknowledgments

We thank the anonymous reviewers for their extremely fruitful comments.

## References

[1] P.V.C. Hough, A Method and Means for Recognizing Complex Patterns, U.S. Patent 3,069,654, December 18, 1962.
[2] A. Rosenfeld, Picture processing by computer, ACM Comput. Surv. 1 (September(3)) (1969) 147–176.
[3] R.O. Duda, P.E. Hart, Use of the Hough Transformation to detect lines and curves in pictures, Commun. ACM 15 (January(1)) (1972) 11–15.
[4] P.M. Merlin, D.J. Farber, A parallel mechanism for detecting curves in pictures, IEEE Trans. Comput. (January(1)) (1975) 96–98.
[5] G.C. Stockman, A.K. Agrawala, Equivalence of Hough curve detection to template matching, Commun. ACM 20 (November(11)) (1977) 820–822.
[6] S.D. Shapiro, Feature space transforms for curve detection, Pattern Recognit. 10 (3) (1978) 129–143.
[7] S.D. Shapiro, Properties of transforms for the detection of curves in noisy images, Comput. Graph. Image Process. 8 (2) (1978) 219–236.
[8] S. Tsuji, F. Matsumoto, Detection of ellipses by a modified Hough Transform, IEEE Trans. Comput. c-27 (August(8)) (1978) 777–781.
[9] D.H. Ballard, Generalizing the Hough Transform to detect arbitrary shapes, Pattern Recognit. 13 (2) (1981) 111–122.
[10] S.R. Deans, Hough transform from the Radon transform, IEEE Trans. Pattern Anal. Mach. Intell. 2 (1981) 185–188.
[11] J. O'Rourke, Dynamically quantized spaces for focusing the Hough transform, in: The Seventh IJCAI, Vancouver, 1981, pp. 737–739.
[12] K.R. Sloan, Dynamically quantized pyramids, in: The Seventh IJCAI, Vancouver, 1981, pp. 734–736.

[13] T.M. van Veen, F.C.A. Groen, Discretization errors in the Hough Transform, Pattern Recognit. 14 (1) (1981) 137–145.
[14] C.M. Brown, Inherent noise and bias in the Hough Transform, IEEE Trans. Pattern Anal. Mach. Intell. PAMI-5 (September(5)) (1983).
[15] C.R. Dyer, Gauge inspection using Hough transform, IEEE Trans. Pattern Anal. Mach. Intell. 5 (November) (1983) 621–623.
[16] M. Kushnir, K. Abe, K. Matsumoto, An application of the Hough transform to the recognition of printed Hebrew characters, Pattern Recognit. 16 (2) (1983) 183–191.
[17] A. Wallace, Grayscale image processing for industrial applications, Image Vis. Comput. 1 (4) (1983) 178–188.
[18] L. Dorst, A.W.M. Smeulders, Discrete representation of straight lines, IEEE Trans. Pattern Anal. Mach. Intell. PAMI-6 (July(4)) (1984) 450–463.
[19] H. Hakalahti, D. Harwood, L.S. Davis, Two-dimensional object recognition by matching local properties of contour points, Pattern Recognit. Lett. 2 (4) (1984) 227–234.
[20] T.M. Silberberg, L. Davis, D. Harwood, An iterative Hough procedure for three-dimensional object recognition, Pattern Recognit. 17 (6) (1984) 621–629.
[21] T.M. Silberbberg, The Hough transform on the geometric arithmetic parallel processor, in: IEEE Conference on Computer Architecture for Pattern Analysis and Image Database Management, 1985, pp. 387–393.
[22] E.R. Davies, Image space transforms for detecting straight edges in industrial images, Pattern Recognit. Lett. 4 (July(3)) (1986) 185–192.
[23] H. Li, M.A. Lavin, Fast Hough transform based on the bintree data structure, in: IEEE CVPR Conference, Miami Beach, 1986, pp. 640–642.
[24] H. Li, M.A. Lavin, R.J. LeMaster, Fast Hough transform: a hierarchical approach, Comput. Vis. Graph. Image Process. 36 (2) (1986) 139–161.
[25] H. Maitre, Contribution to the prediction of performance of the Hough transform, IEEE Trans. Pattern Anal. Mach. Intell. 8 (5) (1986) 669–674.
[26] F. Natterer, The Mathematics of Computerized Tomography, BG Teubner, Stuttgart, 1986.
[27] W.B. Baringer, B.C. Richards, R.W. Brodersen, J. Sanz, D. Petkovic, A VLSI implementation of PPPE for real-time image processing in radon space-work in progress, in: Computer Architecture for Pattern Analysis and Machine Intelligence (CAPAMI), 1987, pp. 88–93.
[28] M.A. Fischler, O. Firschein, Parallel guessing: a strategy for high speed computation, Pattern Recognit. 20 (2) (1987) 257–263.
[29] J. Illingworth, J. Kittler, The adaptive Hough Transform, IEEE Trans. Pattern Anal. Mach. Intell. PAMI-9 (September(5)) (1987) 690–698.
[30] J.L.C. Sanz, I. Dinstein, D. Petkovic, Computing multi-coloured polygonal masks in pipeline architectures and its application to automated vision inspection, Commun. ACM 30 (April(4)) (1987) 318–329.
[31] A. Cross, G. Wadge, Geological lineament detection using the Hough Transform, in: Proceedings of IGARSS, IEEE, August 1988, pp. 1779–1782.
[32] L64250 HHP, Histogram/Hough Transform Processor, LSI Logic Corporation, 1988.
[33] K. Hanahara, T. Maruyama, T. Uchiyama, A real-time processor for the Hough transform, IEEE Trans. Pattern Anal. Mach. Intell. 10 (January(1)) (1988) 121–125.
[34] J. Illingworth, J. Kittler, A survey of the Hough Transform, Comput. Vis. Graph. Image Process. 44 (1) (1988) 87–116.
[35] M.H. Kim, H.Y. Hwang, D.S. Cho, A relaxation approach to the Hough Transform, in: The Seventh Annual International Phoenix Conference on Computers and Communications, IEEE, 1988, pp. 485–489.
[36] J.L. Krahe, P. Pousset, The detection of parallel straight lines with the application of the Hough Transform, in: The Ninth International Conference on Pattern Recognition, vol. 2, IEEE, 1988, pp. 939–941.
[37] W. Lie, Y. Chen, Line drawing extraction of polyhedrons using polarized Hough Transform, in: The 14th Annual Conference of Industrial Electronics Society, IEEE, 1988, pp. 86–91.
[38] D. Ben-Tzvi, A.A. Naqvi, M. Sandler, Efficient parallel implementation of the Hough transform on a distributed memory system, Image Vis. Comput. 7 (3) (1989) 167–172.
[39] A. Califano, R.M. Bolle, R.W. Taylor, Generalized neighborhoods: a new approach to complex parameter feature extraction, in: IEEE Computer Society Conference on Computer Vision and Pattern Recognition (CVPR), IEEE, 1989, pp. 192–199.
[40] F. Cheng, W. Hsu, M. Chen, Recognition of handwritten chinese characters by modified Hough Transform techniques, IEEE Trans. Pattern Anal. Mach. Intell. 11 (April(4)) (1989) 429–439.
[41] A.L. Fisher, P.T. Highman, Computing the Hough transform on a scan line array processor, IEEE Trans. Pattern Anal. Mach. Intell. March(11) (3) (1989) 262–265.
[42] D.D. Haule, A.S. Malowany, Object recognition using fast adaptive Hough Transform, in: IEEE Pacific Rim Conference on Communications, Computers and Signal Processing, June 1989, pp. 91–94.
[43] E.S. McVey, G.L. Dempsey, J. Garcia, R.M. Inigo, Artificial neural network implementation of the Hough Transform, in: The 23rd Asilomar Conference on Signals, Systems and Computers, IEEE, 1989, pp. 128–132.
[44] H. Muammar, M. Nixon, Approaches to extending the Hough Transform, in: IEEE International Conference on Acoustics, Speech and Signal Processing (ICASSP), 1989, pp. 1556–1559.
[45] T. Risse, Hough transform for line recognition: complexity of evidence accumulation and cluster detection, Comput. Vis. Graph. Image Process. 46 (3) (1989) 327–345.
[46] I.D. Svalbe, Natural representation for straight lines and the Hough Transform on discrete arrays, IEEE Trans. Pattern Anal. Mach. Intell. 11 (September (9)) (1989) 941–950.
[47] D. Timmermann, H. Hahn, Hough Transform using Cordic method, Electron. Lett. 25 (February(3)) (1989) 205–206.
[48] H.K. Yuen, J. Illingworth, J. Kittler, Detecting partially occluded ellipses using the Hough Transform, Image Vis. Comput. 7 (1) (1989) 31–37.
[49] D. Cyganski, W.F. Noel, J.A. Orr, Analytic Hough transform, in: Society of Photo-Optical Instrumentation Engineers (SPIE) Conference Series, vol. 1260, 1990, pp. 148–159.
[50] W. Eric, L. Grimson, D.P. Huttenlocher, On the sensitivity of the Hough Transform for object recognition, IEEE Trans. Pattern Anal. Mach. Intell. 12 (March(3)) (1990) 255–274.
[51] U. Eckhardt, G. Maderlechner, A general approach for parametrizing the Hough transform, in: Proceedings of the 10th International Conference on Pattern Recognition, IEEE, vol. 1, 1990, pp. 626–630.
[52] N.D. Franics, G.R. Nudd, T.J. Atherton, D.J. Kerbyson, R.A. Packwood, J. Vaudin, Performance evaluation of the hierarchical Hough transform on an associative M-SIMD architecture, in: Proceedings of the 10th International Conference on Pattern Recognition, IEEE, vol. 2, 1990, pp. 509–511.
[53] D.J. Hunt, L.W. Nolte, A.R. Reibman, W.H. Ruedger, Hough transform and signal detection theory performance for images with additive noise, Comput. Vis. Graph. Image Process. 52 (3) (1990) 386–401.
[54] V.F. Leavers, Active intelligent vision using the dynamic generalized Hough Transform, in: Proceedings of the British Machine Vision Conference, 1990, pp. 49–54.
[55] J. Koplowitz, M. Lindenbaum, A. Bruckstein, The number of digital straight lines on an $N \times N$ grid, IEEE Trans. Inf. Theory 36 (1) (1990) 192–197.
[56] L. Xu, E. Oja, P. Kultanen, A new curve detection method: randomized Hough transform (RHT), Pattern Recognit. Lett. 11 (5) (1990) 331–338.
[57] M.E. Brummer, Hough Transform detection of the longitudinal fissure in tomographic head images, IEEE Trans. Med. Imaging 10 (March(1)) (1991) 74–81.
[58] J.R. Bergen, H. Shvaytser, A Probabilistic algorithm for computing Hough Transforms, J. Algorithms 12 (4) (1991) 639–656.
[59] A. Beinglass, H.J. Wolfson, Articulated object recognition, or: how to generalize the generalized Hough transform, in: Proceedings of IEEE Computer Society Conference on Computer Vision and Pattern Recognition (CVPR), IEEE, 1991, pp. 461–466.
[60] R. Chan, W.C. Siu, New parallel Hough Transform for circles, Comput. Digit. Tech. IEE Proc. E 138 (September(5)) (1991) 335–344.
[61] S. Jeng, W. Tsai, Scale and orientation-invariant generalized Hough Transform—a new approach, Pattern Recognit. 24 (11) (1991) 1037–1051.
[62] N. Kiryati, A.M. Bruckstein, Antialiasing the Hough Transform, CVGIP: Graph. Models Image Process. 53 (May(3)) (1991) 213–222.
[63] N. Kiryati, Y. Eldar, A.M. Bruckstein, A probabilistic Hough Transform, Pattern Recognit. 24 (4) (1991) 303–316.
[64] N. Kiryati, M. Lindenbaum, A.M. Bruckstein, Digital or analog Hough transform? Pattern Recognit. Lett. 12 (5) (1991) 291–297.
[65] C. Kang, R. Park, K. Lee, Extraction of straight line segments using rotation transformation: generalized Hough Transformation, Pattern Recognit. 24 (7) (1991) 633–641.
[66] Y. Liu, D. Cyganski, R.F. Vaz, An efficient implementation of the analytic Hough transform for exact linear feature extraction, Proc. Intell. Robots Comput. Vis. X: Algorithms Tech. (1991) 298–309.
[67] S.Y.K. Yuen, V. Hlavac, An approach to quantization of Hough space, in: Proceedings of the Seventh Scandinavian Conference on Image Analysis, 1991, pp. 733–740.
[68] M. Atiquzzaman, Multiresolution Hough Transform: an efficient method of detecting patterns in images, IEEE Trans. Pattern Anal. Mach. Intell. 14 (November(11)) (1992) 1090–1095.
[69] C.K. Chan, M.B. Sandler, A neural network shape recognition system with Hough transform input feature space, in: International Conference on Image Processing and its Applications, IET, 1992, pp. 197–200.
[70] H. Kalviainen, E. Oja, L. Xu, Randomized hough transform applied to translational and rotational motion analysis, in: Proceedings of the 11th IAPR International Conference on Pattern Recognition, vol. I. Conference A: Computer Vision and Applications, IEEE, 1992, pp. 672–675.
[71] J. Princen, J. Illingworth, J. Kittler, A formal definition of the Hough Transform: properties and relationships, J. Math. Imaging Vis. 1 (2) (1992) 153–168.
[72] P.L. Palmer, J. Kittler, M. Petrou, A Hough transform algorithm with a 2D hypothesis testing kernel, in: The 11th International Conference on Speech and Signal Analysis, 1992, pp. 276–279.
[73] D.C.W. Pao, H.F. Li, R. Jayakumar, Shapes recognition using the straight line Hough Transform: theory and generalization, IEEE Trans. Pattern Anal. Mach. Intell. 14 (November(11)) (1992) 1076–1089.
[74] P.-K. Ser, W.-C. Siu, Sampling Hough algorithm for the detection of lines and curves, in: Proceedings of IEEE International Symposium on Circuits and Systems (ISCAS), vol. 5, IEEE, 1992, pp. 2497–2500.
[75] T. Wada, T. Matsuyama, $\gamma$–$\omega$ Hough Transform—elimination of quantization noise and linearization of voting curves in the $\rho$–$\theta$ parameter space, in: International Conference on Pattern Recognition, IEEE, 1992, pp. 272–275.
[76] B. Frischmuth, K. Frischmuth, U. Eckhardt, On Invariance of the Projected Radon Transform, Inst. f. Angewandte Mathematik d. Univ. Hamburg, 1993.

Please cite this article as: P. Mukhopadhyay, B.B. Chaudhuri, A survey of Hough Transform, Pattern Recognition (2014), http://dx.doi.org/10.1016/j.patcog.2014.08.027

[77] V.F. Leavers, Survey: which Hough Transform? CVGIP: Image Underst. 58 (September(2)) (1993) 250–264.
[78] D.N.K. Leung, L.T.S. Lam, W.C.Y. Lam, Diagonal quantization for the Hough transform, Pattern Recognit. Lett. 14 (March(3)) (1993) 181–189.
[79] S.M. Bhandarkar, A fuzzy probabilistic model for the generalized Hough Transform, IEEE Trans. Syst. Man Cybern. 24 (May(5)) (1994) 745–759.
[80] D. Chang, S. Hashimoto, An inverse voting algorithm for Hough transform, in: IEEE International Conference on Pattern Recognition (ICIP), vol. 1, 1994, pp. 223–227.
[81] J.H. Han, L. Koczy, T. Poston, Fuzzy Hough transform, Pattern Recognit. Lett. 15 (7) (1994) 649–658.
[82] L. Lin, V.K. Jain, Parallel architectures for computing the Hough transform and CT image reconstruction, in: Proceedings of IEEE International Conference on Application Specific Array Processors, IEEE, 1994, pp. 152–163.
[83] J. Princen, Hypothesis testing: a framework for analyzing and optimizing Hough Transform performance, IEEE Trans. Pattern Anal. Mach. Intell. 16 (April(4)) (1994) 329–341.
[84] J. Radon, Uber die Bestimmung von Funktionen durch ihre Integralwerte längs gewisser Mannigfaltigkeiten (On the determination of functions by their integral values along certain manifolds), 75 years of Radon transform (Vienna, 1992), in: Conference Proceedings and Lecture Notes in Mathematical Physics, vol. IV, International Press, Cambridge, MA, 1994, pp. 324–339.
[85] V.A. Shapiro, V.H. Ivanov, Real-time Hough/Radon transform: algorithm and architectures, in: International Conference on Image Processing, IEEE, vol. 3, 1994, pp. 630–634.
[86] D. Ioannou, Using the Hough transform for determining the length of a digital straight line segment, Electron. Lett. 31 (May(10)) (1995) 782–784.
[87] D.J. Kerbyson, T.J. Atherton, Circle Detection using Hough Transform Filters, Image Processing and its Applications, IEE, no. 410, July 1995.
[88] H. Kalviainen, P. Hirvonen, L. Xu, E. Oja, Probabilistic and non-probabilistic Hough transforms: overview and comparisons, Image Vis. Comput. 13 (May (4)) (1995) 239–252.
[89] M.-J. Li, R.-W. Dai, A personal handwritten Chinese character recognition algorithm based on the generalized Hough Transform, in: Proceedings of the Third International Conference on Document Analysis and Recognition, IEEE, vol. 2, 1995, pp. 828–831.
[90] L. Likforman-Sulem, A. Hanimyan, C. Faure, A Hough based algorithm for extracting text lines in handwritten documents, in: Proceedings of the Third International Conference on Document Analysis and Recognition, IEEE, vol. 2, 1995, pp. 774–777.
[91] P.K. Ser, W.C. Siu, A new generalized Hough Transform for the detection of irregular objects, J. Vis. Commun. Image Represent. 6 (September(3)) (1995) 256–264.
[92] R.C. Agrawal, R.K. Shevgaonkar, S.C. Sahasrabudhe, A fresh look at the Hough transform, Pattern Recognit. Lett. 17 (10) (1996) 1065–1068.
[93] J.D. Bruguera, N. Guil, T. Lang, J. Villalba, E.L. Zapata, Cordic based parallel/pipelined architecture for the Hough transform, J. VLSI Signal Process. Syst. Signal Image Video Technol. 12 (3) (1996) 207–221.
[94] V. Chatzis, I. Pitas, Select and split fuzzy cell Hough transform—a fast and efficient method to detect contours in images, in: Proceedings of the Fifth IEEE International Conference on Fuzzy Systems, vol. 3, September 1996, pp. 1892–1898.
[95] B. Gatos, S.J. Perantonis, N. Papamarkos, Accelerated Hough transform using rectangular image decomposition, Electron. Lett. 32 (8) (1996) 730–732.
[96] P.-F. Fung, W.-S. Lee, I. King. Randomized generalized Hough transform for 2-D gray scale object detection, in: Proceedings of the 13th International Conference on Pattern Recognition, vol. 2, IEEE, 1996, pp. 511–515.
[97] H. Kalviainen, Motion detection using the randomized Hough Transform: exploiting gradient information and detecting multiple moving objects, IEE Proc. Vis. Image Signal Process. 143 (December(6)) (1996) 361–369.
[98] J. Kneip, P. Pirsch, Memory efficient list based Hough Transform for programmable digital signal processors with on-chip caches, in: Digital Signal Processing Workshop Proceedings, IEEE, 1996, pp. 191–194.
[99] R.A. McLaughlin, Randomized Hough Transform: better ellipse detection, in: IEEE TENCON—Digital Signal Processing Applications, vol. 1, 1996, pp. 409–414.
[100] M. Nakanishi, T. Ogura, A real-time CAM-based Hough Transform algorithm and its performance evaluation, in: IEEE Proceedings of ICPR, 1996.
[101] S. Pavel, S.G. Akl, Efficient algorithms for the Hough Transform on arrays with reconfigurable optical buses, in: Proceedings of the 10th International Parallel Processing Symposium (IPP), IEEE, 1996, pp. 697–701.
[102] P.A. Toft, J.A. Sørensen, The Radon transform—theory and implementation (PhD dissertation), Technical University of Denmark (Danmarks Tekniske Universitet), Center for Bachelor of Engineering Studies (Center for Diplomingeniøruddannelse), Center for Information Technology and Electronics (Center for Informationsteknologi og Elektronik), 1996.
[103] V. Chatzis, I. Pitas, Randomized fuzzy cell Hough Transform, in: Proceedings of the Sixth IEEE International Conference on Fuzzy Systems, vol. 2, 1997, pp. 1185–1190.
[104] H. Kalviainen, P. Hervonen, An extension to the randomized Hough transform exploiting connectivity, Pattern Recognit. Lett. 18 (1) (1997) 77–85.
[105] R.C. Lo, W.H. Tsai, Perspective-transformation-invariant generalized Hough Transform for perspective planar shape detection and matching, Pattern Recognit. 30 (3) (1997) 383–396.
[106] J.M. Nash, J.N. Carter, M.S. Nixon, The velocity Hough transform: a new technique for dynamic feature extraction, in: Proceedings of the International Conference on Image Processing, IEEE, vol. 2, 1997, pp. 386–389.
[107] A. Samal, J. Edwards, Generalized Hough transform for natural shapes, Pattern Recognit. Lett. 18 (5) (1997) 473–480.
[108] D.M. Tsai, An improved generalized Hough transform for the recognition of overlapping objects, Image Vis. Comput. 15 (12) (1997) 877–888.
[109] T.Y. Tian, M. Shah, Recovering 3D motion of multiple objects using Adaptive Hough Transform, IEEE Trans. Pattern Anal. Mach. Intell. 19 (October(10)) (1997) 1178–1183.
[110] F. Vajda, Implementation issues of the Hough Transform, J. Syst. Archit. 43 (1) (1997) 163–165.
[111] M.C.K. Yang, J.S. Lee, C.C. Lien, C.L. Huang, Hough Transform modified by line connectivity and line thickness, IEEE Trans. Pattern Anal. Mach. Intell. 19 (August(8)) (1997) 905–910.
[112] J. Immerkaer, Some remarks on the straight line Hough transform, Pattern Recognit. Lett. 19 (12) (1998) 1133–1135.
[113] D. Ioannou, E.T. Dugan, A note on "A fresh look at the Hough Transform", Pattern Recognit. Lett. 19 (1998) 307–308.
[114] S.J. Perantonis, N. Vassilas, Th. Tsenoglou, K. Seretis, Robust line detection using weighted region based Hough transform, Electron. Lett. 34 (April(7)) (1998) 648–650.
[115] T. Tuytelaars, L.V. Gool, M. Proesmans, T. Moons, The cascaded Hough transform as an aid in aerial image interpretation, in: The Sixth International Conference on Computer Vision, IEEE, 1998, pp. 67–72.
[116] J. Basak, S.K. Pal, Hough Transform network, Electron. Lett. 35 (April(7)) (1999) 577–578.
[117] O. Chutatape, L. Guo, A modified Hough transform for line detection and its performance, Pattern Recognit. 32 (2) (1999) 181–192.
[118] C.-P. Chau, W.-C. Siu, Generalized dual-point Hough transform for object recognition, in: Proceedings of International Conference on Image Processing (ICIP), IEEE, vol. 1, 1999, pp. 560–564.
[119] L. Guo, O. Chutatape, Influence of discretization in image space on Hough transform, Pattern Recognit. 32 (4) (1999) 635–644.
[120] C. Galamhos, J. Matas, J. Kittler, Progressive probabilistic Hough transform for line detection, in: IEEE Computer Society Conference on Computer Vision and Pattern Recognition, vol. 1, IEEE, 1999.
[121] D. Ioannou, W. Huda, A.E. Laine, Circle recognition through a 2D Hough Transform and radius histogramming, Image Vis. Comput. 17 (1999) 15–26.
[122] H. Ma, Huiye, Z. Yu, An enhanced skew angle estimation technique for binary document images, in: Proceedings of the Fifth International Conference on Document Analysis and Recognition (ICDAR), IEEE, 1999, pp. 165–168.
[123] C.F. Olson, Constrained Hough Transforms for curve detection, Comput. Vis. Image Underst. 73 (March(3)) (1999) 329–345.
[124] R. Shpilman, V. Brailovsky, Fast and robust techniques for detecting straight line segments using local models, Pattern Recognit. Lett. 20 (9) (1999) 865–877.
[125] N. Kiryati, H. Kälviäinen, S. Alaoutinen, Randomized or probabilistic Hough transform: unified performance evaluation, Pattern Recognit. Lett. 21 (13) (2000) 1157–1164.
[126] T.C. Chen, K.L. Chung, An efficient randomized algorithm for detecting circles, Comput. Vis. Image Underst. 83 (2) (2001) 172–191.
[127] C. Galambos, J. Kittler, J. Matas, Gradient based progressive probabilistic Hough transform, in: IEE Proceedings on Vision, Image and Signal Processing, vol. 148, no. 3, IET, 2001, pp. 158–165.
[128] L. Iocchi, D. Mastrantuono, D. Nardi, A probabilistic approach to Hough localization, in: Proceedings of the International Conference on Robotics and Automation (ICRA), IEEE, vol. 4, 2001, pp. 4250–4255.
[129] Q. Ji, R.M. Haralick, Error propagation for the Hough transform, Pattern Recognit. Lett. 22 (6) (2001) 813–823.
[130] P. Lappas, J.N. Carter, R.I. Damper, Object tracking via the dynamic velocity Hough Transform, in: Proceedings of the International Conference on Image Processing, IEEE, vol. 2, 2001, pp. 371–374.
[131] K. Maharatna, S. Banerjee, A VLSI array architecture for Hough transform, Pattern Recognit. 34 (7) (2001) 1503–1512.
[132] G. Olmo, E. Magli, All-integer Hough Transform: performance evaluation, in: International Conference on Image Processing, IEEE, vol. 3, 2001, pp. 338–341.
[134] S. Tagzout, K. Achour, O. Djekoune, Hough transform algorithm for FPGA implementation, Signal Process. 81 (6) (2001) 1295–1301.
[135] T. Achalakul, S. Madarasmi, A concurrent modified algorithm for generalized Hough transform, in: IEEE International Conference on Industrial Technology (ICIT), vol. 2, IEEE, 2002, pp. 965–969.
[136] N. Bonnet, An unsupervised generalized Hough transform for natural shapes, Pattern Recognit. 35 (5) (2002) 1193–1196.
[137] P. Bhattacharya, A. Rosenfeld, I. Weiss, Point-to-line mappings as Hough transforms, Pattern Recognit. Lett. 23 (14) (2002) 1705–1710.
[138] A. Epstein, G.U. Paul, B. Vettermann, C. Boulin, F. Klefenz, A parallel systolic array ASIC for real-time execution of the Hough Transform, IEEE Trans. Nucl. Sci. 49 (April(2)) (2002) 339–346.
[139] A. Kimura, T. Watanabe, An extension of the generalized Hough transform to realize affine-invariant two-dimensional (2D) shape detection, in: The 16th International Conference on Pattern Recognition, IEEE, vol. 1, 2002, pp. 65–69.
[140] A. Leich, H.J. Jentschel, Projection transform with discretization noise suppression, in: The Sixth International Conference on Signal Processing, vol. 2, IEEE, 2002, pp. 1071–1074.

Please cite this article as: P. Mukhopadhyay, B.B. Chaudhuri, A survey of Hough Transform, Pattern Recognition (2014), http://dx.doi.org/10.1016/j.patcog.2014.08.027

[141] D. Walsh, A.E. Raftery, Accurate and efficient curve detection in images: the importance sampling Hough transform, Pattern Recognit. 35 (2002) 1421–1431.
[142] Q. Li, Y. Xie, Randomised Hough transform with error propagation for line and circle detection, Pattern Anal. Appl. 6 (1) (2003) 55–64.
[143] A.A. Rad, K. Faez, N. Qaragozlou, Fast circle detection using gradient pair vectors, in: DICTA, 2003, pp. 879–888.
[144] R. Strzodka, I. Ihrke, M. Magnor, A Graphics Hardware implementation of the generalized Hough transform for fast object recognition, scale, and 3D pose detection, in: Proceedings of the 12th International Conference on Image Analysis and Processing (ICIAP), IEEE, 2003, pp. 188–193.
[145] Z. Cheng, Y. Liu, Efficient technique for ellipse detection using restricted randomized Hough transform, in: Proceedings of International Conference on Information Technology: Coding and Computing, ITCC, vol. 2, IEEE, 2004, pp. 714–718.
[146] M. van Ginkel, C.L.L. Hendriks, L.J. van Vliet, A Short Introduction to the Radon and Hough Transforms and How They Relate to Each Other, The Quantitative Image Group Technical Report Series, N. QI-2004-01, 2004, pp. 1–9.
[147] R. Klette, A. Rosenfeld, Digital straightness—a review, Discrete Appl. Math. 139 (2004) 197–230.
[149] J. Qi, Z. Shi, X. Zhao, Y. Wang, A novel fingerprint matching method based on the Hough transform without quantization of the Hough space, in: The Third International Conference on Image and Graphics, IEEE, 2004, pp. 262–265.
[150] Q.-C. Tian, Q. Pan, Y.-M. Cheng, Q.-X. Gao, Fast algorithm and application of Hough transform in iris segmentation, in: Proceedings of International Conference on Machine Learning and Cybernetics, IEEE, vol. 7, 2004, pp. 3977–3980.
[151] N.B. Amor, N.E.B. Amara, Multifont arabic character recognition using Hough transform and Hidden Markov models, in: Proceedings of the Fourth International Symposium on Image and Signal Processing and Analysis (ISPA), IEEE, 2005, pp. 285–288.
[152] A. Bonci, T. Leo, S. Longhi, A Bayesian approach to the Hough transform for line detection, IEEE Trans. Syst. Man Cybern. Part A: Syst. Hum. 35 (November(6)) (2005) 945–955.
[153] J. Basak, S.K. Pal, Theoretical quantification of shape distortion in fuzzy Hough transform, Fuzzy Sets Syst. 154 (2005) 227–250.
[154] C.A. Basca, M. Talos, R. Brad, Randomized Hough transform for ellipse detection with result clustering, in: International Conference on Computer as a Tool, EUROCON, IEEE, vol. 2, 2005, pp. 1397–1400.
[155] S. Golemati, J. Stoitsis, T. Balkizas, K.S. Nikita, Comparison of B-Mode, M-Mode and Hough transform methods for measurement of arterial diastolic and systolic diameters, in: Proceedings of the 27th Annual Conference on Engineering in Medicine and Biology, IEEE, 2005, pp. 1758–1761.
[156] L. Li, Z. Feng, K. He, A randomized algorithm for detecting multiple ellipses based on least square approach, Opto-Electron. Rev. 13 (1) (2005) 61–67.
[157] A.N. Marana, A.K. Jain, Ridge-based fingerprint matching using Hough transform, in: The 18th Brazilian Symposium on Computer Graphics and Image Processing, IEEE, 2005, pp. 112–119.
[158] K. Mayasandra, S. Salehi, W. Wang, H.M. Ladak, A distributed arithmetic hardware architecture for real-time Hough transform based segmentation, Can. J. Electr. Comput. Eng. (4) (2005) 201–205.
[159] P. Shivakumara, G. Hemantha Kumar, D.S. Guru, P. Nagabhushan, A new boundary growing and Hough transform based approach for accurate skew detection in binary document images, in: Proceedings of International Conference on Intelligent Sensing and Information Processing (ICISIP), IEEE, 2005, pp. 140–146.
[160] J. Song, M.R. Lyu, A Hough transform based line recognition method utilizing both parameter space and image space, Pattern Recognit. 38 (2005) 539–552.
[161] N. Aggarwal, W.C. Karl, Line detection in images through regularized Hough transform, IEEE Trans. Image Process. 15 (3) (2006) 582–591.
[162] J. Cha, R.H. Cofer, S.P. Kozaitis, Extended Hough transform for linear feature detection, Pattern Recognit. 39 (2006) 1034–1043.
[163] E. Duquenoy, A. Taleb-Ahmed, Applying the Hough transform pseudo-linearity property to improve computing speed, Pattern Recognit. Lett. 27 (2006) 1893–1904.
[164] S.-Y. Guo, X.-F. Zhang, F. Zhang, Adaptive randomized Hough transform for circle detection using moving window, in: Proceedings of the Fifth International Conference on Machine Learning and Cybernetics, IEEE, August 2006, pp. 3880–3885.
[165] F. Li, M.K.H. Leung, Hierarchical identification of palmprint using line-based Hough transform, in: The 18th International Conference in Pattern Recognition (ICPR), IEEE, vol. 4, 2006, pp. 149–152.
[166] V. Shapiro, Accuracy of the straight line Hough transform: the non-voting approach, Comput. Vis. Image Underst. 103 (2006) 1–21.
[167] Y. Tong, H. Wang, D. Pi, Q. Zhang, Fast algorithm of Hough transform-based approaches for fingerprint matching, in: The Sixth World Congress on Intelligent Control and Automation (WCICA), IEEE, vol. 2, 2006, pp. 10425–10429.
[168] S.R. Deans, The Radon Transform and Some of its Applications, Courier Dover Publications, 2007.
[169] H. Duan, X. Liu, H. Liu, A nonuniform quantization of Hough space for the detection of straight line segments, in: The Second International Conference on Pervasive Computing and Applications (ICPCA), IEEE, 2007, pp. 149–153.
[171] Y. Li, S. Zhu, Modified Hough transform for iris location, in: International Conference on Control and Automation (ICCA), IEEE, 2007, pp. 2630–2632.
[172] K. Nishimoto, A. Sagami, K. Kaneyama, Three dimensional recognition of environments for a mobile robot using laser range finder, in: SICE Annual Conference, IEEE, 2007, pp. 401–405.
[173] S. Touj, N.E.B. Amara, H. Amiri, Two approaches for arabic script recognition-based segmentation using the Hough Transform, in: The ninth International Conference on Document Analysis and Recognition (ICDAR), IEEE, vol. 2, IEEE, 2007, pp. 654–658.
[174] N. Toronto, B.S. Morse, D. Ventura, K. Seppi, The Hough transform's implicit Bayesian foundation, in: International Conference on Image Processing, IEEE, vol. 4, 2007, pp. IV–377.
[175] L. Xu, A unified perspective and new results on RHT computing, mixture based learning, and multi-learner based problem solving, Pattern Recognit. 40 (2007) 2129–2153.
[176] F. Xu, Y-Q. Jin, Automatic reconstruction of building objects from multiaspect meter-resolution SAR images, IEEE Trans. Geosci. Remote Sens. 45 (July(7)) (2007) 2336–2353.
[177] O. Ecabert, J. Peters, H. Schramm, C. Lorenz, J. von Berg, M.J. Walker, Automatic model-based segmentation of the heart in CT images, IEEE Trans. Med. Imaging 27 (September(9)) (2008) 1189–1201.
[178] S.-Y. Guo, Y.-G. Kong, Q. Tang, F. Zhang, Probabilistic Hough Transform for line detection utilizing surround suppression, in: Proceedings of the Seventh International Conference on Machine Learning and Cybernetics, July 2008, pp. 2993–2998.
[179] F.J. Jaime, J. Hormigo, J. Villalba, E.L. Zapata, SIMD enhancements for a Hough Transform implementation, in: The 11th EUROMICRO Conference on Digital System Design Architectures, Methods and Tools, IEEE, 2008, pp. 899–903.
[180] W. Lu, J. Tan, Detection of incomplete ellipse in images with strong noise by iterative randomized Hough transform (IRHT), Pattern Recognit. 41 (2008) 1268–1279.
[181] W. Min, Z. Yanning, Hough Transform relative nonuniform parameter space for the detection of line segments, in: International Conference on Computer Science and Software Engineering, IEEE, vol. 1, 2008, pp. 764–767.
[182] R.K. Satzoda, S. Suchitra, T. Srikanthan, Parallelizing the Hough transform computation, IEEE Signal Process. Lett. 15 (2008) 297–300.
[183] Y. Chen, M. Adjouadi, C. Han, A. Barreto, A new unconstrained iris image analysis and segmentation method in biometrics, in: International Symposium on Biomedical Imaging: From Nano to Macro (ISBI), IEEE, 2009, pp. 13–16.
[184] R. Dahyot, Statistical Hough Transform, IEEE Trans. Pattern Anal. Mach. Intell. August(31) (8) (2009) 1502–1509.
[185] S. Ensafi, M. Eshghi, M. Naseri, Recognition of separate and adjoint Persian letters using primitives, in: IEEE Symposium on Industrial Electronics and Applications, ISIEA, vol. 2, IEEE, 2009, pp. 611–616.
[186] H. Fei, G. Yanling, W. Lili, A new ellipse detector based on Hough Transform, in: The Second International Conference on Information and Computing Science, IEEE, 2009, pp. 301–305.
[187] S. Guo, T. Pridmore, Y. Kong, X. Zhang, An improved Hough transform voting scheme utilizing surround suppression, Pattern Recognit. Lett. 30 (2009) 1241–1252.
[188] P.E. Hart, How the Hough Transform was invented, IEEE Signal Process. Mag. (November) (2009) 18–22.
[189] H. Izadinia, F. Sadeghi, M.M. Ebadzadeh, Fuzzy generalized Hough Transform invariant to rotation and scale in noisy environment, in: Fuzzy IEEE, 2009, pp. 153–158.
[190] L. Xu, E. Oja, Randomized Hough Transform, Encyclopaedia of Artificial intelligence (3 volumes), IGI Global (IGI) Publishing Company, 2009.
[191] W. Xiangyu, S. Ramanathan, M. Kankanhalli, A robust framework for aligning lecture slides with video, in: The 16th International Conference on Image Processing (ICIP), IEEE, 2009, pp. 249–252.
[192] C.-H. Chuang, Y.-C. Lo, C.-C. Chang, S.-C. Cheng, Multiple object motion detection for robust image stabilization using block-based Hough transform, in: The Sixth International Conference on Intelligent Information Hiding and Multimedia Signal Processing, IEEE, 2010, pp. 623–626.
[193] B. Dai, Y. Pan, H. Liu, D. Shi, S. Sun, An improved RHT algorithm to detect line segments, in: International Conference on Image Analysis and Signal Processing (IASP), IEEE, 2010, pp. 407–410.
[194] S. Du, B.J. Wyk, C. Tu, X. Zhang, An improved Hough Transform neighborhood map for straight line segments, IEEE Trans. Image Process. 19 (March(3)) (2010) 573–585.
[195] D. Duan, M. Xie, Q. Mo, Z. Han, Y. Wan, An improved Hough transform for line detection, in: International Conference on Computer Application and System Modeling (ICCASM), vol. 2, IEEE, 2010, pp. V2-354.
[196] H. Ghodrati, M.J. Dehghani, M.S. Helfroush, K. Kazemi, Localization of noncircular iris boundaries using morphology and arched Hough transform, in: The Second International Conference on Image Processing Theory, Tools and Applications (IPTA), 2010, pp. 458–463.
[197] D. Graovac, S. Juric-Kavelj, I. Petrovic, Mobile robot pose tracking by correlation of laser range finder scans in Hough domain, in: The 19th International Workshop on Robotics, IEEE, 2010, pp. 273–278.
[198] G.-Q. Jiang, C.-J. Zhao, Y.-S. Si, A machine vision based crop rows detection for agricultural robots, in: Proceedings of the International Conference on Wavelet Analysis and Pattern Recognition, IEEE, 2010, pp. 114–118.
[199] D.R. Shashi Kumar, K. Kiran Kumar, K.B. Raja, R.K. Chhotaray, S. Pattnaik, Hybrid fingerprint matching using block filer and strength factors, in: The Second International Conference on Computer Engineering and Applications (ICCEA), IEEE, vol. 1, 2010, pp. 476–480.

Please cite this article as: P. Mukhopadhyay, B.B. Chaudhuri, A survey of Hough Transform, Pattern Recognition (2014), http://dx.doi.org/10.1016/j.patcog.2014.08.027

ARTICLE IN PRESS



[200] C. Tong, S. Kamata, 3D object matching based on spherical Hilbert scanning, in: Proceedings of the 17th International Conference on Image Processing (ICIP), IEEE, 2010, pp. 2941–2944.
[201] F. Tombari, L.D. Stefano, Object recognition in 3D scenes with occlusions and clutter by Hough voting, in: The Fourth Pacific-Rim Symposium on Image and Video Technology (PSIVT), IEEE, 2010, pp. 349–355.
[202] X. Zhang, J. Tian, K. Deng, Y. Wu, X. Li, Automatic liver segmentation using a statistical shape model with optimal surface detection, IEEE Trans. Biomed. Eng. 57 (October(10)) (2010) 2622–2626.
[203] B. Epshtein, Determining document skew using inter-line spaces, in: International Conference on Document Analysis and Recognition (ICDAR), IEEE, 2011, pp. 27–31.
[204] L. Fei, J. Bo, L.H. Wei, F. Bo, Cross-range scaling of interferometric ISAR based on randomized Hough Transform, in: International Conference on Signal Processing, Communications and Computing (ICSPCC), IEEE, 2011, pp. 1–4.
[205] R.F.C. Guerreiro, P.M.Q. Aguiar, Incremental local Hough Transform for line segment extraction, in: The 18th IEEE International Conference on Image Processing (ICIP), IEEE, 2011, pp. 2841–2844.
[206] Y.-P. Gao, Y.-M. Li, Z. Hu, Skewed text correction based on the improved Hough transform, in: International Conference on Image Analysis and Signal Processing (IASP), IEEE, 2011, pp. 368–372.
[207] P.P. Guan, H. Yan, Blood cell image segmentation based on the Hough transform and fuzzy curve tracing, in: Proceedings of the International Conference on Machine Learning and Cybernetics, IEEE, July 2011, pp. 1696–1701.
[208] F. Haghjoo, A.R. Mallahzadeh, V. Riazi, A.S. Heikhi, Noncoherent integration of HRR RADAR signals for detection of fluctuating targets in non Gaussian clutter using the hough transform, in: CIE International Conference on Radar (Radar), vol. 1, IEEE, 2011, pp. 502–506.
[209] Y. Ito, K. Ogawa, K. Nakano, Fast ellipse detection algorithm using Hough Transform on the GPU, in: The Second International Conference on Networking and Computing, IEEE, 2011, pp. 313–319.
[210] Y.J. Kim, M. Park, D.-H. Lee, J.-Y. Lee, J.-J. Lee, Vision based direction determination of a mobile robot in indoor environment, in: The Fifth International Conference on Digital Ecosystems and Technologies (DEST), IEEE, 2011, pp. 153–157.
[211] A.A. Paulino, J. Feng, A.K. Jain, Latent fingerprint matching using descriptor-based Hough Transform, in: International Joint Conference on Biometrics (IJCB), IEEE, 2011, pp. 1–7.
[212] X. Tian, W. Chao, H. Zhang, F. Wu, Extraction and analysis of structural features of ships in high resolution SAR images, in: CIE International Conference in Radar (Radar), vol. 1, IEEE, 2011, pp. 630–633.
[213] P. Tino, H. Zhao, H. Yan, Searching for coexpressed genes in three-color cDNA microarray data using a probabilistic model-based Hough Transform, IEEE/ACM Trans. Comput. Biol. Bioinform. 8 (4) (2011) 1093–1107.
[214] K.L. Chung, Y.H. Huang, S.M. Shen, A.S. Krylov, D.V. Yurin, E.V. Semeikina, Efficient sampling strategy and refinement strategy for randomized circle detection, Pattern Recognit. 45 (2012) 252–263.
[215] Z.-H. Chen, A.W. Su, M.-T. Sun, Resource-efficient FPGA architecture and implementation of hough transform, IEEE Trans. Very Large Scale Integr. Syst. 20 (8) (2012) 1419–1428.
[216] J. Dai, J. Feng, J. Zhou, Robust and efficient ridge-based palmprint matching, IEEE Trans. Pattern Anal. Mach. Intell. 34 (August(8)) (2012) 1618–1632.
[217] L. Jiang, Efficient randomized Hough transform for circle detection using novel probability sampling and feature points, Optik 123 (2012) 1834–1840.
[218] N.A. Jalil, R. Sahak, A. Saparon, A comparison of iris localization techniques for pattern recognition analysis, in: The Sixth Asia Modelling Symposium (AMS), IEEE, 2012, pp. 75–80.
[219] J.E. McManigle, R.V. Stebbing, J.A. Noble, Modified Hough transform for left ventricle myocardium segmentation in 3-D echocardiogram images, in: The Ninth International Symposium in Biomedical Imaging (ISBI), IEEE, 2012, pp. 290–293.
[220] J. Zhang, J. Wu, X. Shi, Y. Zhang, Estimating vertebral orientation from biplanar radiography based on contour matching, in: The 25th International Symposium on Computer-Based Medical Systems (CBMS), IEEE, 2012, pp. 1–5.

Please cite this article as: P. Mukhopadhyay, B.B. Chaudhuri, A survey of Hough Transform, Pattern Recognition (2014), http://dx.doi.org/10.1016/j.patcog.2014.08.027